Coordination Chemistry Reviews 279 (2014) 96–114

Contents lists available at ScienceDirect

Coordination Chemistry Reviews

journal homepage: www.elsevier.com/locate/ccr

Review

The application of electrospray ionization mass spectrometry to homogeneous catalysis

Krista L. Vikse, Zohrab Ahmadi, J. Scott McIndoe*

Department of Chemistry, University of Victoria, P.O. Box 3065, Victoria, BC V8W 3V6, Canada

Contents

ARTICLE INFO

Article history:
Received 4 February 2014
Accepted 13 June 2014
Available online 20 June 2014

Keywords:
Organometallic
Homogeneous catalysis
Mechanism
Electrospray ionization mass spectrometry

ABSTRACT

Electrospray ionization mass spectrometry (ESI-MS) is increasingly being used as a tool to gain mechanistic insights into homogeneous metal-catalyzed reactions. Here we briefly discuss the advantages of ESI-MS for studying solution-phase reactions and review the work that has been conducted in the area to date. In order to investigate any catalytic system by ESI-MS all species of interest must be charged: either inherently, adventitiously or intentionally by installing a charged or chargeable tag. This review will be organized accordingly. In addition, a portion of the review is devoted to the emerging use of ESI-MS to collect continuous kinetic data on reactants, products and reactive intermediates by in situ, real-time analysis of catalytic reaction mixtures. The review covers work in the field up to 2013.

1. Introduction

Metal-catalyzed reactions are a proven and powerful tool in the endeavour to address future energy needs and to develop modern materials. However, in order to fully capitalize on the potential benefits of these types of reactions more detailed information is required on the workings of metal catalysts under their normal operating conditions. Electrospray ionization mass spectrometry (ESI-MS) can provide access to mechanistic information that is difficult or even impossible to attain using standard spectroscopic techniques. There are a number of things that make mass spectrometry, and especially ESI-MS, well suited to the study of products, reactants and catalytic intermediates in metal-catalyzed reactions: ESI-MS is a soft technique that operates on solutions and can leave weak bonding interactions intact; only species that are already charged in solution or contain an easily charged site are detected, so most common solvents are "invisible" and very low detection limits are accessible [1,2]; analysis is fast (on the order of seconds), and intermediates at nanomolar concentrations can be detected with ease; finally, since each species in solution is usually represented by a single peak in the mass spectrum, it is relatively simple to extract information from complex mixtures.

A growing body of literature exists in which investigators have taken advantage of these attributes of ESI-MS to study organometallic systems. The first was Berman who used ESI-MS to detect a number of environmentally important organoarsenic ions [3]. Another notable early example comes from Canty in 1993 who reported the positive ESI-MS and tandem MS studies of various palladium and platinum organometallic complexes [4]. Since then, the primary use of ESI-MS in the area of solution-phase organometallic chemistry has been in the identification of short-lived, low concentration intermediates from catalytic mixtures. Towards this end, ESI-MS has been used to study catalytic oxidations [5–8], hydrogenations [9–11], hydrosilylations

* Corresponding author. Tel.: +1 250 721 7181; fax: +1 250 721 7147.
E-mail address: mcindoe@uvic.ca (J. Scott McIndoe).

http://dx.doi.org/10.1016/j.ccr.2014.06.012
0010-8545/

[12] and carbon-carbon bond-forming [13–15] reactions with the most attention given to palladium-catalyzed carbon–carbon bond-forming reactions [14,16–21]. A number of book chapters have been written on the subject of ESI-MS analysis of organometallic reaction intermediates [22–24] and this review aims to highlight more recent advances and new directions in the field.

It is important to mention that a range of mass spectrometry techniques also exist which allow organometallic ions of interest to be isolated and studied directly in the gas phase. These methods contribute significantly to the utility of mass spectrometry as a mechanistic tool in organometallic chemistry, but this review will focus solely on reactions occurring in homogeneous solutions. For an overview of gas-phase studies of organometallic complexes see the excellent reviews by Traeger [25], Plattner [26], Holčapek [27] and Schröder [28]. New advances in the field of ion spectroscopy deserve mention; namely, the detailed *structural* characterization of reactive intermediates within a mass spectrometer [29].

In order to investigate any catalytic system by ESI-MS all species of interest must be charged; either inherently, adventitiously (e.g. by protonation or loss of a halide) or intentionally by installing a charged or chargeable tag: the studies discussed will be organized accordingly. It is worth noting that although most investigations to date have focused on palladium or ruthenium systems there is no inherent limitation to which metals can be investigated by ESI-MS as long as the species are charged. The final part of this review is devoted to the emerging use of ESI-MS to collect continuous real-time kinetic data on catalytic transformations including direct kinetic analysis of individual elementary reaction steps.

2. Inherently-charged systems

Reactions with inherently charged intermediates allow for straightforward analysis – the standard reaction mixture can simply be sampled and infused directly into the mass spectrometer. Oxidation reactions lend themselves particularly well to this method of analysis since the reaction intermediates are often inherently charged. A range of manganese-containing intermediates for a variety of reactions have been observed and the groups of Bortolini [30,5,31,32] and Smith [33,7,34] have been strong contributors to research in this area.

Among the first reports was the investigation of an iron-catalyzed oxidation system in 1997. ESI-MS was used to characterize the intermediate $[Fe^{III}\text{-TPA(OOH)}]^{2+}$ in the stereospecific hydroxylation of alkanes by hydrogen peroxide (TPA, tris(2-pyridyl-methyl)amine) [35]. It is unique among oxidation reactions studied by ESI-MS in that all other reports address manganese- or vanadium-catalyzed systems.

In 1998 evidence for the existence of a commonly invoked intermediate for a variety of oxygen transfer reactions involving the $[O=Mn^{V}]$ moiety was obtained by interception of an $[O=Mn^{V}(salen)(OIPh)]^{+}$ complex (Fig. 1A) and a binuclear $[\mu\text{-}O(Mn^{IV}(salen)(OIPh))_2]^{2+}$ complex (Fig. 1B) [36]. Later, an ESI-MS study on the Mn-catalyzed oxidative kinetic resolution of secondary alcohols by $PhI(OAc)_2$ reported the observation of a similar manganese salen intermediate $[Mn^{V}(salen)(PhIO)(OCH(CH_3)Ph]^{+}$ (Fig. 1C) [6]. This, along with the observation of $[Mn^{III}(salen)(PhI(OAc)_2)]^{+}$ (Fig. 1D), allowed the proposal of a possible catalytic cycle for the kinetic resolution of secondary alcohols by this system.

Mn-MeTACN complexes have been studied extensively by ESI-MS in the oxidation of a variety of organic substrates using hydrogen peroxide (MeTACN = 1,4,7-trimethyl-1,4,7-triazacyclononane). An assortment of binuclear and mononuclear species has been observed [7,33,34]. One such example focused on the use of these complexes for the oxidative drying of alkyd paints. The binuclear

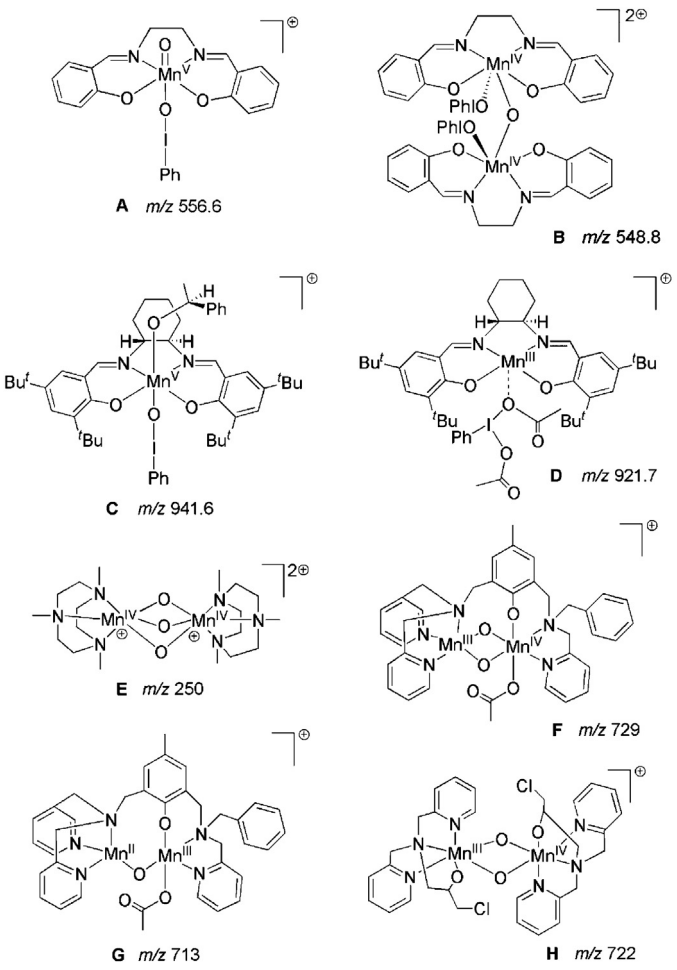

Fig. 1. Manganese-containing species observed by ESI(+)-MS.

complex, $[Mn_2^{IV}(\mu\text{-}O)_3MeTACN)_2]^{2+}$ (Fig. 1E), was shown to be an effective catalyst; in this case for oxidation of ethyl linoleate (a model complex for alkyd resins) [37]. From a solution of $[Mn_2^{IV}(\mu\text{-}O)_3MeTACN_2][PF_6]_2$ and hydroperoxide, peaks corresponding to the starting material $[Mn_2^{IV}(\mu\text{-}O)_3MeTACN_2]^{2+}$ were initially dominant and small peaks corresponding to the mixed valent binuclear system $[Mn^{IV}Mn^{III}(\mu\text{-}O)_3MeTACN_2]^{+}$ were present. After 24 h peaks corresponding to the reduced $[Mn_2^{III}(\mu\text{-}O)_2MeTACN_2]^{2+}$ dominated the spectrum, consistent with the catalyst acting to decompose hydroperoxides via a reversible equilibrium between $Mn(IV)_2/Mn(IV)Mn(III)/Mn(III)_2$ (Scheme 1). In alkyd paints this decomposition of hydroperoxides leads to the formation of volatile aldehyde products which aid in the drying of the oil paint.

Isotope labelling experiments are a valuable tool in the mass spectrometrist's mechanistic toolbox for confirming peak assignment and clarifying mechanistic details. For example, the mechanism of peroxide disproportionation by various dimanganese complexes was investigated by Dubois et al. using ESI-MS. Proposed active species of the forms bis(μ-oxo)dimanganese(III/IV)

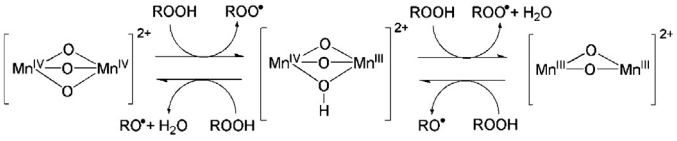

Scheme 1. Proposed catalytic cycle for the decomposition of hydroperoxide by Mn-MeTACN based on ESI-MS studies.
Modified from reference [37].

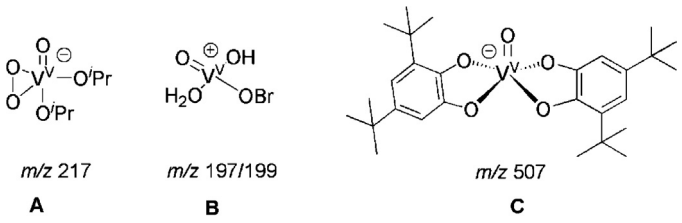

Fig. 2. Vanadium-containing species observed by ESI(-)-MS and ESI(+)-MS.

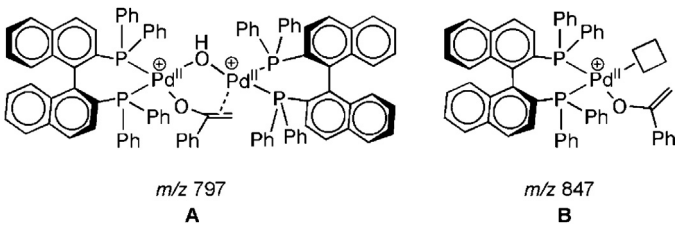

Fig. 3. Bi- and mono-nuclear palladium ions observed by ESI(+)-MS and proposed as catalytic intermediates in the enantioselective Manich-type reaction of enol silyl ethers with N-aryl-iminoacetic acid esters [42].

(Fig. 1F, *m/z* 729) and (μ-oxo)dimanganese(II/III) (Fig. 1G, *m/z* 713) were observed in each case and confirmed by isotope labelling ESI-MS studies. For the intermediate containing two oxygen atoms, ^{18}O labelling experiments confirmed that both oxygen atoms come from the same hydrogen peroxide molecule. An overall mechanism was proposed [38,39].

The use of ESI-MS to complement more traditional reactivity studies is highlighted in a report on manganese-based peroxidase and catalase activity which appeared in 2009. Based on ESI-MS experiments and supported by UV–vis and EPR experiments, the binuclear manganese intermediate $[(PClNOL)Mn^{III}\text{-}(\mu\text{-}O)_2\text{-}Mn^{IV}(PClNOL)]^+$ (Fig. 1H, *m/z* 722) was identified and proposed to be responsible for the catalase-like activity of the manganese(II) compound $[Mn^{II}(HPClNOL)(\eta_1\text{-}NO_3)(\eta_2\text{-}NO_3)]$ HPClNOL = $N((CH_2)C_5H_4N)_2(CH_2(CH)OH(CH_2)Cl)$ [40].

The few vanadium-based studies present in the literature are summarized briefly here and, as with the manganese systems, they focus on the identification of key intermediates in vanadium-catalyzed oxidations. These cases readily illustrate the importance of considering both the positive and negative ion modes of ESI-MS when probing reaction mixtures.

In 2001, negative ion ESI-MS studies suggested that monoperoxovanadium species are responsible for the vanadium-catalyzed oxidation of isopropyl alcohol to acetone [30]. Fragmentation studies conducted in the gas phase showed loss of acetone from the species $[OV(O_2)(O^iPr)_2]^-$ (Fig. 2A, *m/z* 217), confirming that the reaction occurs within the inner sphere of the metal. In a follow-up study, positive ion ESI-MS lead to the observation of the intermediate $[VO(OH_2)(OH)(OBr)]^+$ (Fig. 2B, *m/z* 197/199), which was implicated as a potential intermediate in the vanadium-catalyzed oxidation of bromide by hydrogen peroxide [32].

In 2005, a selection of pre-catalysts were employed in the vanadium-catalyzed oxygenation of 3,5-ditert-butylcatechol. ESI-MS experiments that were conducted on the post-reaction solutions led to the detection of two common negative ions: $[VO(DTBC)_2]^-$ (Fig. 2C) and $[V(DTBC)_3]^-$ (DTBC = 3,5-di-tert-butylcatecholate dianion) [41]. Through kinetic experiments the species corresponding to $[V(DTBC)_3]^-$ was ruled out as the catalytically active species and the neutral species that was shown to correspond to $[VO(DTBC)_2]^-$, namely $(VO(DBSQ)(DTBC))_2$ (DBSQ = 3,5-di-tert-butylsemiquinone anion), was reported as a common catalyst for this reaction. While this study describes an adventitiously-charged system (the proposed active catalyst is in fact neutral), it is described here along with the other vanadium-catalyzed systems for cohesion.

As opposed to most oxidation reactions, palladium-catalyzed carbon–carbon bond-forming reactions generally proceed through neutral intermediates, but there are some exceptions. An early example is the detection of a binuclear Pd complex (Fig. 3A) identified by ESI-MS in 1999 and proposed in the enantioselective Manich-type reaction of enol silyl ethers with N-aryl-iminoacetic acid esters. A potentially active mononuclear species (Fig. 3B) with a vacant coordination site was also observed and a mechanism for the reaction was outlined based on these two species [42]. Care was taken in the experimental design to ensure that B was a true solution-phase species and not one formed during the ESI process. A similar and more recent example involves a Michael-type Friedel-Crafts reaction between indoles and chalcones with $FeCl_3$ and $PdCl_2$ additives. The introduction of these two metals at 5 mol% was found to improve the efficiency and lower the cost of the reaction. ESI-MS investigation led to the identification of the

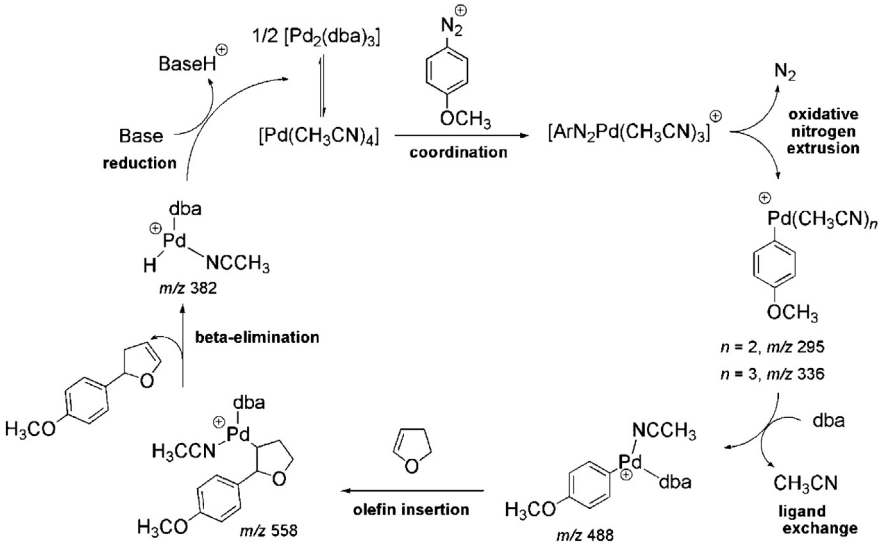

Scheme 2. Proposed mechanism for the Heck reaction with arene diazonium salts based on ESI(+)-MS data, *m/z* values are given for observed cationic species. Modified from reference [17].

potentially responsible species: a bimetallic iron-palladium catalyst of the form $[FePd(chalcone)Cl_5]^+$[43].

Certain aspects of the Heck and Suzuki reactions and one example of a palladium-catalyzed allylic substitution reaction have also lent themselves to ESI-MS analysis via inherently charged intermediates.

In 2004, Matsuda developed a phosphine-free version of the Heck reaction involving arene diazonium salts with $[Pd_2(dba)_3]$.dba as the palladium source [44]. Eberlin studied the system by ESI-MS(/MS) to verify the proposed catalytic cycle [17]. Pd-containing species were directly observed which supported the proposed process involving oxidative nitrogen extrusion, ligand exchange, olefin insertion, and β-hydride elimination (Scheme 2). No species related to a Pd-bound arene diazonium cation were observed, presumably because the intermediate is too short-lived. The species $[(4\text{-}MeOPh)Pd(CH_3CN)(dba)]^+$ (*m/z* 488) becomes dominant in mixture solution of palladium and diazonium salt after 90 min, and subsequent addition of various olefins demonstrated that this species is the most active towards olefin insertion.

Eberlin also studied the Heck reaction of aryltellurides [45] and Svennebring [19] reported the identification of three types of cationic, catalytic intermediates (Fig. 4A–C) in the microwave-assisted, phosphine-containing Heck arylation of electron rich olefins. In the latter case the authors support a Pd(0)/Pd(II) cycle as opposed to a Pd(II)/Pd(IV) cycle based on ESI-MS evidence for reduction of the palladium(II) precatalyst to Pd(0) by the ligand, and oxidative addition of the aryl substrate to a Pd(0) species. None of the expected Pd-bound olefin intermediates were observed; however, this is often the case either because the olefin-bound species is neutral or because OA (oxidative addition) is the turnover-limiting step and the subsequent steps occur too quickly to be observed by the sampling method (in this case sampling included quenching and dilution of samples from a reaction vessel).

In 2007, negative-ion ESI-MS was used to detect the boron species responsible for transmetallation in the Suzuki reaction: $[PhB(OCH_3)_3]^-$ (Fig. 4D) [46]. Soon after, ESI-MS allowed the in situ observation of small catalytically active palladium clusters during a Suzuki reaction that could be precursors to catalytically active palladium nanoparticles. $[(IL)_5Pd_3(H_2O)]^+$, $[(IL)_3Pd_3(H_2O)_7]^+$ and the transmetallation product $[(IL)_2PdAr]^+$ were observed where IL = an imidazolium cation or an *N*-heterocyclic carbene [47].

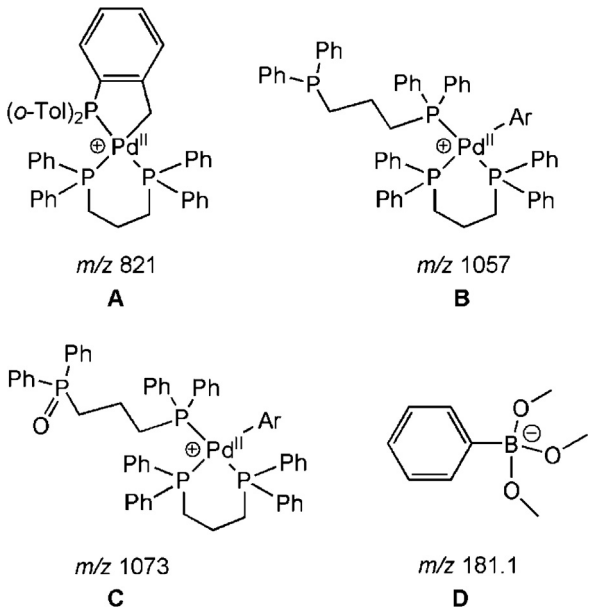

Fig. 4. (A–C) Palladium-containing species observed by ESI-MS and implicated in the microwave-assisted Heck arylation of electron rich olefins.[19] (D) A boron-containing ion implicated in the transmetallation step of the palladium-catalyzed Suzuki cross-coupling reaction [46].

A new method of fast and facile synthesis of aryl ketones from *ortho*-functionalized benzoic acid and nitriles was proposed in 2010. A cationic Pd^{II} complex was used as the catalyst and as opposed to many other Pd catalysts, the charge and oxidation state of Pd does not change over the course of the reaction. This simplified the ESI-MS experiments and allowed the observation of all relevant palladium containing species (Fig. 5). Thus, a mechanistic pathway fully supported by direct experimental evidence was proposed (Scheme 3) [48].

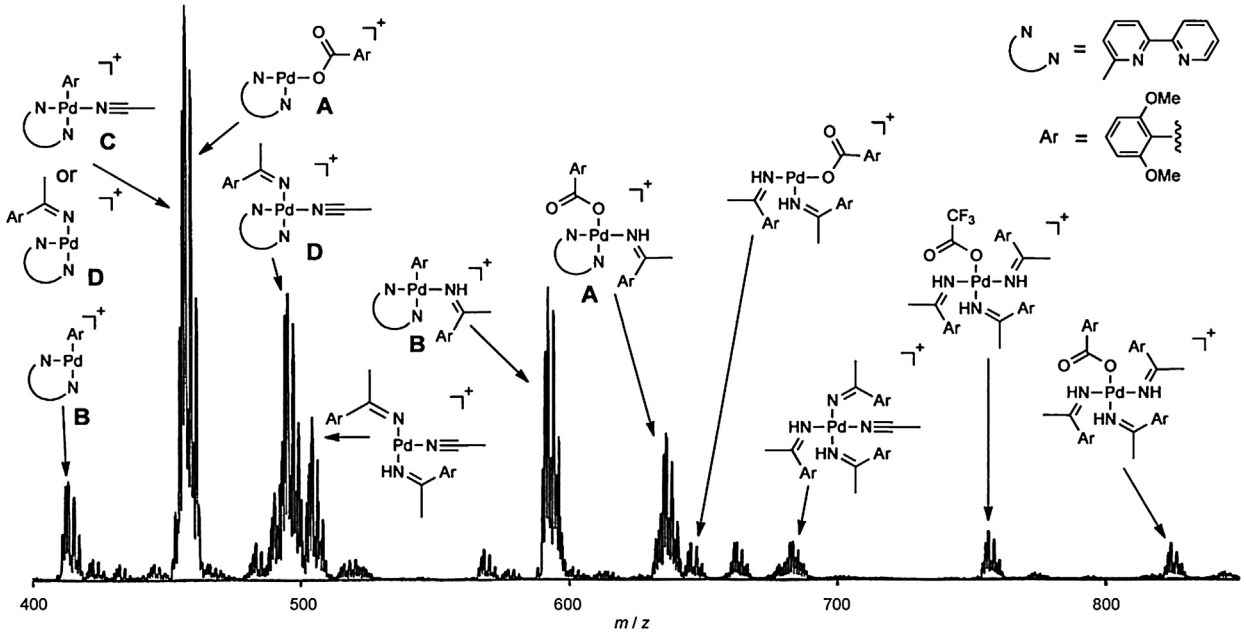

Fig. 5. ESI-MS spectrum for the reaction mixture of 2,6 dimethoxybenzoic acid as the substrate and acetonitrile as the reactant/solvent with using $Pd(O_2CCF_3)_2$. Reprinted with permission from [48]. Copyright ©2010 WILEY-VCH Verlag GmbH & Co. KGaA, Weinheim.

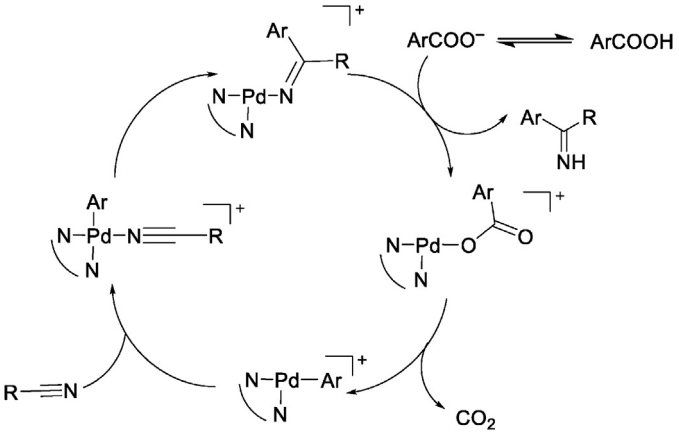

Scheme 3. Proposed mechanistic cycle for palladium-catalyzed decarboxylative addition of benzoic acids to nitriles based on observation of cationic palladium complexes by ESI-MS [48]. R = Me, Et, Pr, Ph, CH_2Ph.

Multinuclear metal complexes that may act as active catalysts or off-cycle species can also be easily identified and studied via ESI-MS. For example, analysis of a simple Pd-catalyzed allylic substitution reaction lead to the discovery of two reversibly formed binuclear bridged palladium complexes (Fig. 6) that act as a reservoir for the active mononuclear catalyst [21]. The observation of dimers when using ESI-MS is common and it is crucial to confirm that they truly exist in solution and are not just formed during the ESI process. In this case the detection was supported by ^{31}P and ^{1}H NMR studies of stoichiometric reaction mixtures and in situ XAFS experiments [49].

Another active binuclear palladium intermediate was reported in 2012 in the Wacker oxidation of alkenes [50]. ESI-MS revealed several binuclear palladium species ligated by the reactant alkene

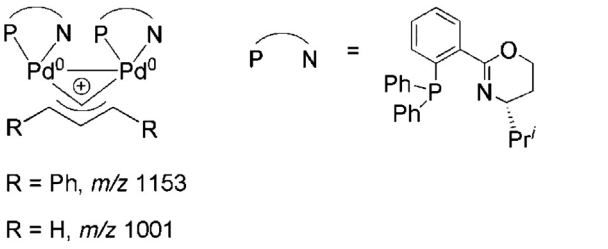

Fig. 6. Two binuclear palladium-bridged allylic complexes discovered by ESI(+)-MS analysis. They are proposed to serve as reservoirs for the active catalyst in a palladium-catalyzed allylic substitution reaction [21].

or the product ketone suggesting that binuclear palladium species play an active role in this transformation. Kinetic experiments performed by GC showed a greater than one dependency of the rate on the concentration of the palladium precursor, which also suggested that binuclear species played a role in the reaction. A mechanism was proposed for this reaction based on these observations. Although there is evidence for the existence of dimeric palladium in many catalytic cycles, in most cases it is still unclear as to whether these species contribute directly to the productive catalytic cycle [51]. ESI-MS studies such as these provide valuable information for understanding the role of such complexes.

In 2013, Pd^{IV} was detected for the first time in oxidative coupling reactions catalyzed by $Pd(OAc)_2$. The intermediacy of Pd^{IV} was proved by collision induced dissociation (CID) studies of analogues of this Pd complex, which produce Pd^{II} through reductive elimination of the product. The effect of different solvents and different anionic ligands was also studied (Scheme 4A). An MS/MS study of an authentic Pd^{IV} complex provided the same fragments as those of the assigned Pd^{IV} intermediates (Scheme 4B) [52].

While ESI-MS studies of systems catalyzed by other metals are less common, one report investigated a ruthenium-catalyzed reaction with naturally charged Ru-cluster intermediates. The

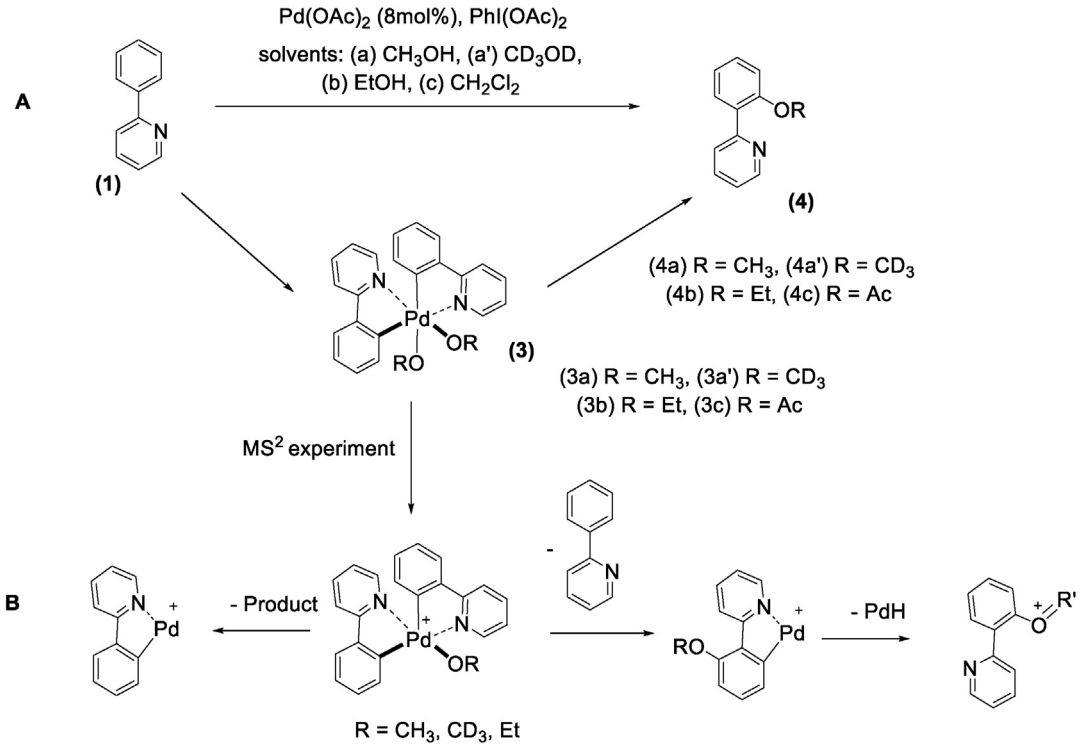

Scheme 4. (A) Proposed mechanism of the palladium-catalyzed 2-phenyl pyridine oxidative coupling reactions. Dependence of intermediates and products to the type of solvents were clearly observed. (B) Observed fragmentation pathways by loss of the product (left) and loss of phenyl pyridine which is followed by dissociation of PdH (right) [52].

cubane structure $[Ru_4(\eta^6\text{-}C_6H_6)_4(OH)_4]^{4+}$ was shown to exist in solution by direct observation of $[Ru_4(\eta^6\text{-}C_6H_6)_4(O)_3(OH)]^+$ [9]. The corresponding dimer $[Ru_2(\eta^6\text{-}C_6H_6)_2(O)(OH)]^+$ was also observed and proposed as the active catalyst in the hydrogenation of benzene.

Direct observation of seven intermediates involved in the hydrosilylation and dehydrogenative silylation of phenylacetylene by an Ir^{II}-NHCtype catalyst allowed the elucidation of both the hydro- and dehydrogenative silylation mechanisms (Scheme 5) [12]. Analysis of fragmentation patterns produced by MS/MS experiments provided insight into the connectivity of species $[I]^+$ and $[III]^+$ where the mass assignment itself was ambiguous. Use of the modified substrate 4-aminophenylacetylene, which is visible by ESI-MS, confirmed formation of the products and indicated the dominant mechanism under each set of reaction conditions.

In 2012 an ESI-MS investigation of Rh-catalyzed [2+2+2] cycloaddition reaction was reported [53]. In this DFT-supported study, several key intermediates were observed and characterized by MS/MS tandem spectrometry. Although reactant and product are neutral, the charged catalyst provided a good opportunity to intercept visible intermediates. A species with *m/z* 974.1 was assigned based on its accurate mass and fragmentation pattern; however, as is often the case with mass spectrometry-based experiments, the authors were unable to distinguish between isomeric structures (Scheme 6).

The copper-catalyzed cross coupling reaction of thiophenol and aryl halide was also studied by ESI-MS. In this study, reported in 2011, three anionic complexes were assigned as key intermediates. Analysis of the same mixture by positive ion mode ESI revealed only the potassium adducts of thiophenol. An anionic

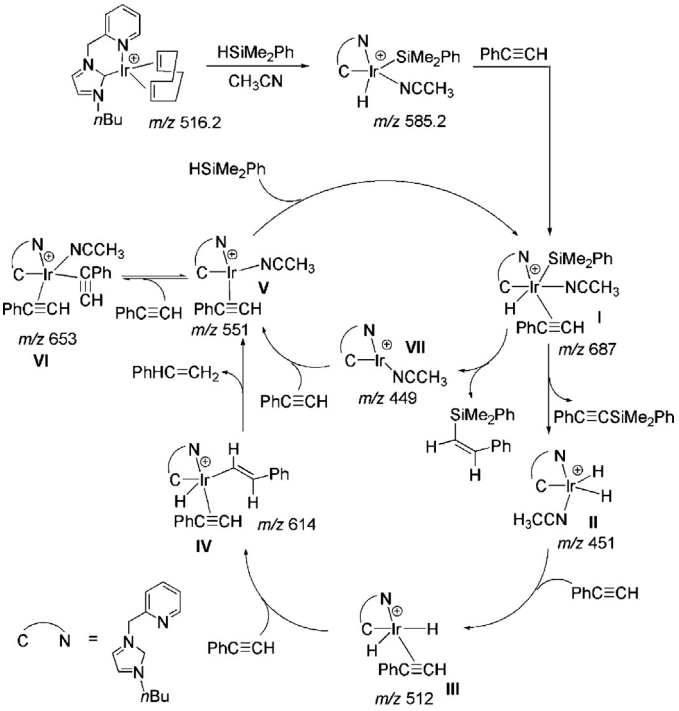

Scheme 5. Proposed mechanisms for the hydrosilylation and dehydrogenative silylation of phenylaceylene by an iridium catalyst, *m/z* values are given for cationic species observed by ESI(+)-MS.
Modified from reference [12].

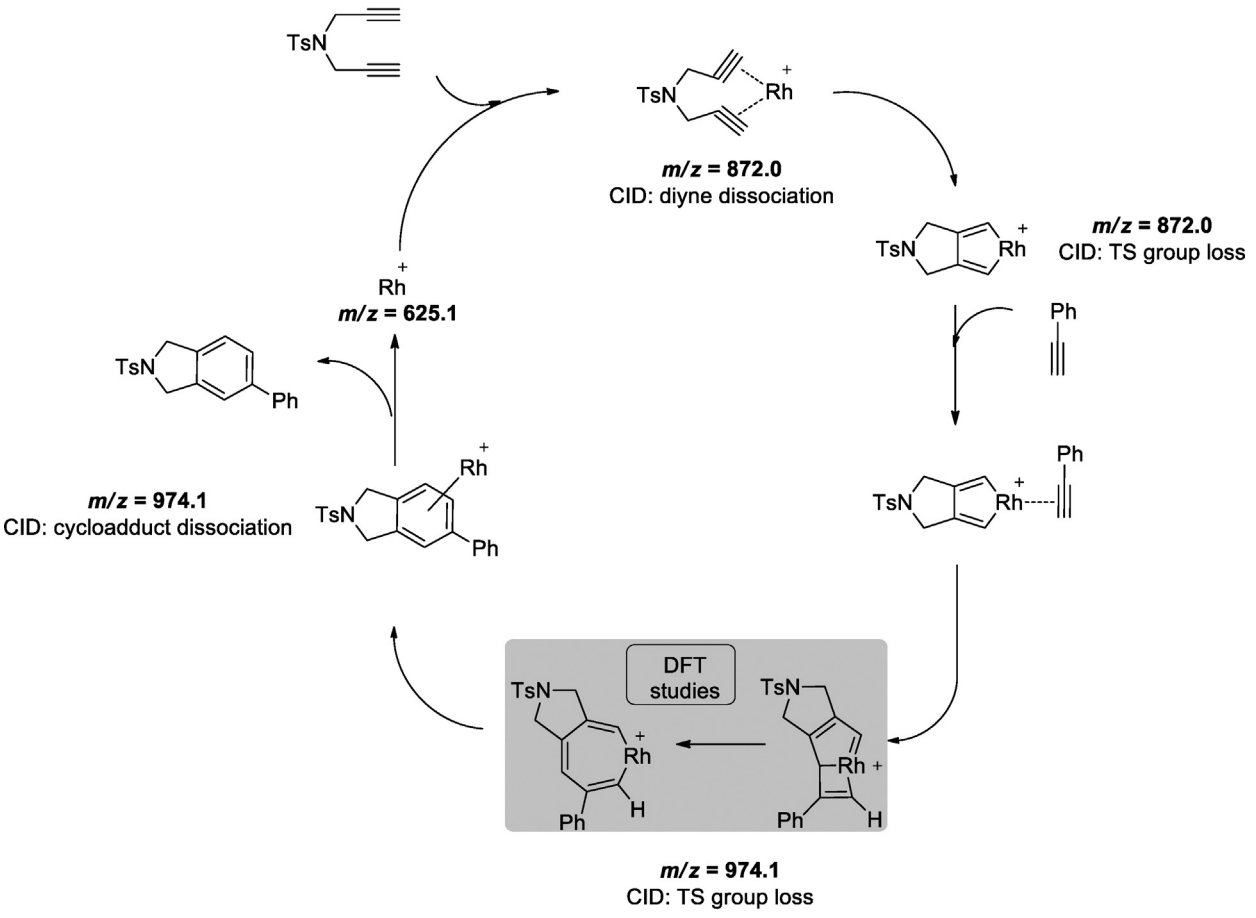

Scheme 6. Rhodim-catalyzed [2+2+2] cycloaddition mechanism for of diynes and monoynes based on detected species by ESI-MS and CID characterization [53].

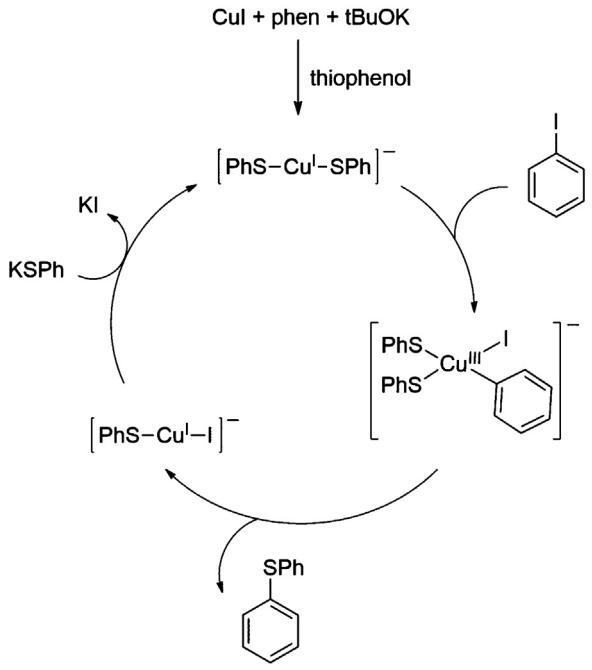

Scheme 7. Suggested catalytic cycle for copper-catalyzed cross coupling reaction of thiophenol and aryl halide based on detected species by ESI-MS [54].

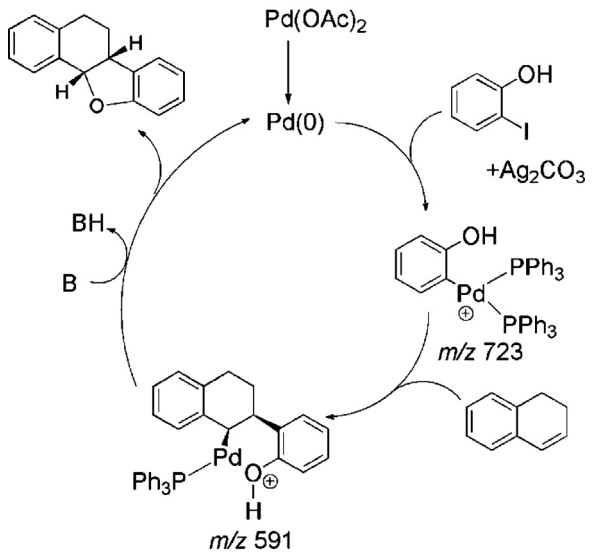

Scheme 8. Proposed mechanism for the oxyarylation of olefins, *m/z* values are given for cationic intermediates observed by ESI(+)-MS. B = base.
Modified from reference [61].

reaction mechanism was proposed based on these observations (Scheme 7) [54].

3. Adventitiously-charged systems

In adventitiously-charged systems intermediates are inherently neutral, but charged species occur without intervention through one or more ionization mechanisms. The most common ionization mechanisms are protonation of a basic site, reversible loss of an anionic ligand like I^- or Br^-, or association of an alkali metal like Na^+ or K^+ (alkali metals are often present as contaminants in mass spectrometers) (Fig. 7). Like inherently charged systems, no modification to the reaction mixture is required. Loss of an anionic ligand, such as in Fig. 7c, is particularly common in organometallic complexes [55] and as a result adventitiously-charged systems were among the first to be investigated by ESI-MS.

A 1993 study on the Raney nickel-catalyzed homo-coupling of 2-bromo-6-methylpyridine allowed for the observation of a number of potentially active catalyst species including the dimer $[(dmbp)Ni(\mu\text{-}Br)_2Ni(dmbp)Br]^+$ through loss of a bromo ligand [13], and in the late 1990s the reactive intermediates in the Ti^{IV}-catalyzed enantioselective sulfoxidation of organic sulfides were extensively analyzed by ESI-MS through protonation of the ligands on titanium [5,31]; however, most subsequent work has focused on palladium-catalyzed or ruthenium-catalyzed reactions.

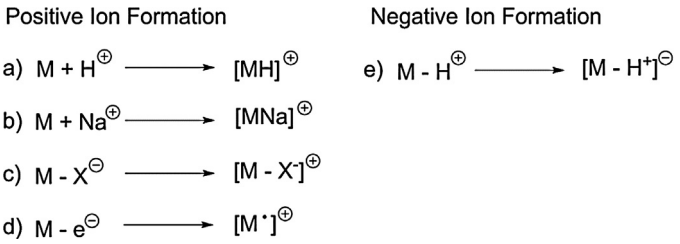

Fig. 7. Common ionization pathways: (a) protonation of a basic site (b) association of a cation to a basic site (c) halide loss (d) oxidation (e) deprotonation of an acidic site.

Early investigations into the mechanism of palladium-catalyzed C–C coupling reactions supported the formation of oxidative addition intermediates in the following cases: when bis-phosphane chelating ligands were employed in the Heck arylation of methyl acrylate (ionized by loss of halide) [56], during the intramolecular cyclization of enamides to form spiro-compounds (ionized by loss of halide) [57] and in the self-coupling of arylboronic acids (ionized by loss of an anionic boron ligand) [58]. In the last case relevant species were also intercepted by protonation of intermediates when the reaction was quenched with trifluoroacetic acid. For example $[Pd(H)(PPh_3)_2(B(OH)(OH_2))]^+$ was detected, a species implicated in the regeneration of the catalyst.

More recently, cationic intermediates have been observed in the Heck reactions of: arene diazonium salts catalyzed by triolefinic macrocycle Pd(0) complexes [17,59], *o*-iodophenols and enoates to form new lactones [60], and *o*-iodophenols with olefins (the *oxa*-Heck reaction) [61]. In the first case ions were formed by oxidation of the analyte at the capillary, or by association of $[NH_4]^+$ or Na^+. In the two other cases ionization occurred through the more typical loss of a halide ligand. The *oxa*-Heck reaction provides a good example of how these experiments are typically performed and the type of information that can be obtained. The oxyarylations of olefins were performed in acetone, catalyzed by palladium, and required the presence of sodium carbonate as base. Samples from the reaction mixtures were diluted with acetonitrile and analyzed by ESI(+)-MS. Loss of iodide after oxidative addition of *o*-iodophenol to palladium afforded positively-charged intermediates. Species consistent with oxidative addition, such as $[Pd(PPh_3)_2(C_6H_5O)]^+$, and the formation of palladacycles of the type seen in Scheme 8 were observed. Based on this, a mechanism for the reaction was proposed (Scheme 8).

A Suzuki cross-coupling reaction between arene diazonium salts and potassium trifluoroborates was studied by ESI-MS in 2007 [16], and used the same triolefinic macrocyclic Pd(0) complex that had been found to catalyze the phosphane-free Heck reaction [17,59]. To further investigate the general mechanism of the reaction, ESI-MS was used to monitor the coupling of $4\text{-}CH_3PhN_2BF_4$ and KBF_3Ph catalyzed by $Pd_2(dba)_3$ in H_2O/CH_3CN. An oxidative addition intermediate was observed along with protonated transmetallation intermediates and homo-coupling intermediates (Scheme 9I, II and III, respectively).

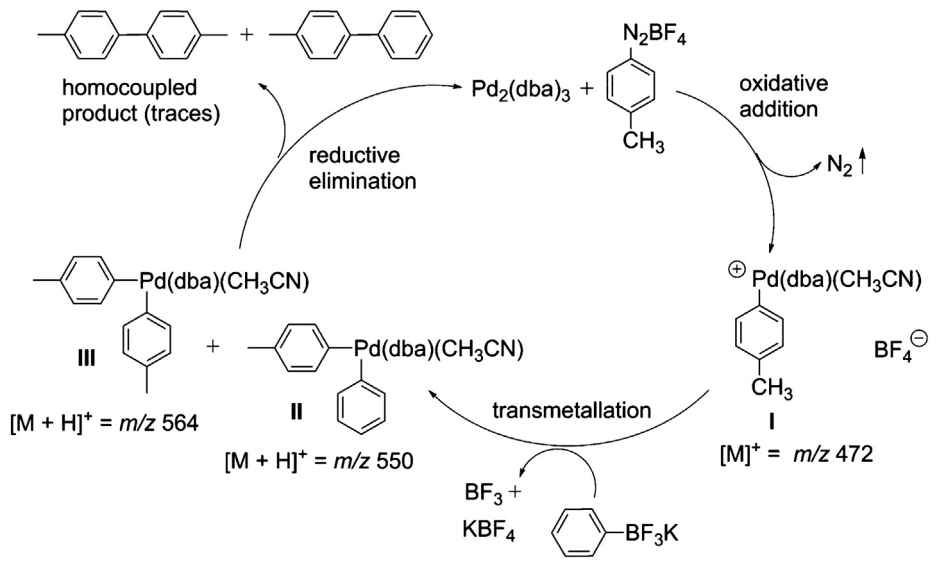

Scheme 9. Proposed mechanism for the Suzuki cross-coupling reaction of arene diazonium salts with potassium organotrifluoroborates based on ESI-MS investigation, *m/z* values are given for cationic intermediates observed by ESI(+)-MS.
Modified from reference [16].

In an ESI-MS monitoring study of the Suzuki-Miyaura reaction using a dichloro-bis(aminophosphine) palladium precatalyst, binuclear Pd complexes were detected after the reaction went to completion, indicating a catalyst sink or a resting state. Addition of starting reagents resumes the reaction, suggesting the active role of the binuclear complex as a reservoir of mononuclear active catalyst. Other interpretations propose the involvement of Pd nanoparticles in which binuclear Pd complexes act as a precursor or perhaps even the active catalyst, but the last possibility seems unlikely. A mechanism for this transformation was proposed based on the intercepted species (Scheme 10) [62].

A 2007 paper by Santos and Eberlin provides an excellent example of a non-innocent ESI process that allows detection of otherwise neutral intermediates [63]. The expected Pd^0 active species for a typical Stille reaction was indirectly observed as its molecular ion $[Pd(PPh_3)_2]^{\bullet+}$. The molecular ion was formed by oxidation of the neutral species at the capillary during the ESI process [63]. The proposed oxidative addition and transmetallation intermediates were also observed, primarily as their molecular ions $[M]^{\bullet+}$. Fig. 8 shows an intermediate undergoing transmetallation. Observation of these Pd-based radical cations provides support for the proposed Stille reaction mechanism; however, care must be taken when examining the behaviour of these radical species in the gas phase since their reactivity is unknown and is unlikely to be the same as their neutral analogues.

The role of Pd^{II} in improving the selectivity of carbon-carbon bond formation in the allylic substitution of 1-acetoxy-1,3-diphenylpropene by acetylacetone in an aqueous system was investigated by Muzart and Roglans (Scheme 11) [15].

Pd^{II} complexes could be seen in both the positive- and negative-ion mode by loss of halide from the metal, or loss of proton from the ligand respectively. In each case, peaks corresponding to the presence of a Pd-enolate complex of the form $[Pd^{II}L(acac)]^+$ ($L = [(HOCH_2CH_2NHCOCH_2)_2NCH_2\text{-}]_2$) (Fig. 9A) were observed while no peaks corresponding to the traditionally-proposed Pd-allyl intermediate were detected (a control was done

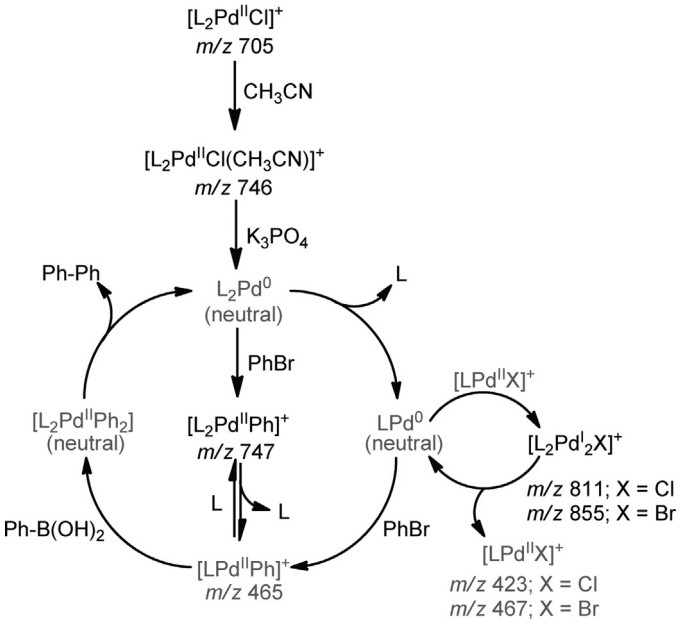

Scheme 10. Proposed mechanistic cycle for Suzuki–Miyaura cross-coupling based on the observation of binuclear palladium complexes. L = 1,1′-(cyclohexylphosphanediyl)dipiperidine.
Reprinted with permission from [62]. Copyright ©2011 American Chemical Society.

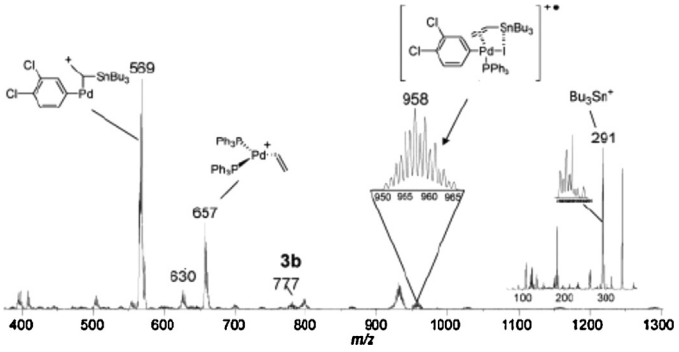

Fig. 8. ESI(+)-MS of the Stille reaction of 3,4-dichloroiodobenzene and vinyltributyltin in acetonitrile mediated by $Pd(PPh_3)_4$. A radical cation intermediate undergoing transmetallation is observed at *m/z* 958.
Reprinted with permission from [64]. Copyright ©2007 American Chemical Society.

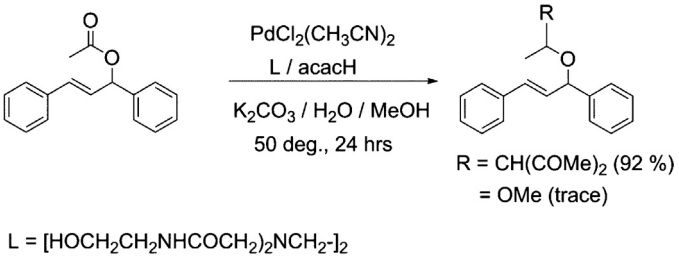

Scheme 11. Allylic substitution of 1-acetoxy-1,3-diphenylpropene by acetylacetone (acacH) [15].

to prove they could see these species using a Pd^0 source). These observations led to the conclusion that the role of palladium is to promote selective nucleophilic attack at the central carbon of the Pd-enolate complex and not to stabilize a Pd-allyl intermediate.

The similar substitution of allylic acetates with sodium *para*-toluenesulfonate using the catalytic mixture $[(\eta^3\text{-allyl})PdCl]_2$ and L (same as above) in aqueous media was also studied by the same group, but with very different results [20]. Peaks were observed corresponding to allyl-type intermediates such as $[PdL(PhCH=CHC(OAc)HCH_3)-OAc]^+$ (Fig. 9B). Two possible mechanisms were proposed based on these observations, one of which involves a Pd^{IV} intermediate.

Some less common Pd-catalyzed bond-forming reactions have been investigated as well, including tellurium–carbon bond formation (ionized by loss of halide) [14], intramolecular nitrogen–carbon bond formation (ionized by association of H^+ or Na^+) [64], and the formation of two new carbon–oxygen bonds in the hydroxyalkoxylation of 2-allylphenols (ionized by loss of H^+ in the negative-ion mode, and loss of an anionic ligand or association of Na^+ in positive-ion mode) [65]. A study by Guo et al. determined the mechanism of a palladium-catalyzed three-component cyclization reaction (the formation of cis-pyrolidine derivatives from imine, iodobenzene and 2-(2,3-allenyl)malonate) [66]. Three key cationic organopalladium species that had lost halide ligands were detected by ESI-FTMS. All ions were characterized by accurate mass determination and subjected to collision induced dissociation to aid in their structural assignment. A carbopalladation mechanism was proposed which takes into account all experimental data (Scheme 12). Oxidative addition of iodobenzene yields the first intermediate, carbopalladation of 2-(2,3-allenyl)malonate gives the second intermediate, and deprotonation and addition of imine leads to the final intermediate. The cycle is completed by intramolecular allylic animation to give the product and the regenerated catalyst. Potassium adducts of the products were also observed to appear as the reaction progressed.

There has been some interest in the study of ruthenium-catalyzed systems. For example, hydrogenation reactions catalyzed by Ru(II)–arene complexes have been the focus of a few ESI-MS studies, the first of which appeared in 2000. In this report, three species (Fig. 10A–C) were detected in a mixture of the

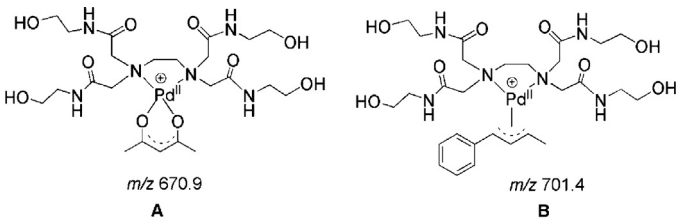

Fig. 9. (A) A Pd-enolate complex observed by ESI(+)-MS during the palladium-catalyzed allylic substitution of 1-acetoxy-1,3-diphenylpropene by acetylacetone [15]. (B) A Pd-allyl complex observed by ESI(+)-MS during the palladium-catalyzed substitution of allylic acetates with sodium *para*-toluenesulfonate [20].

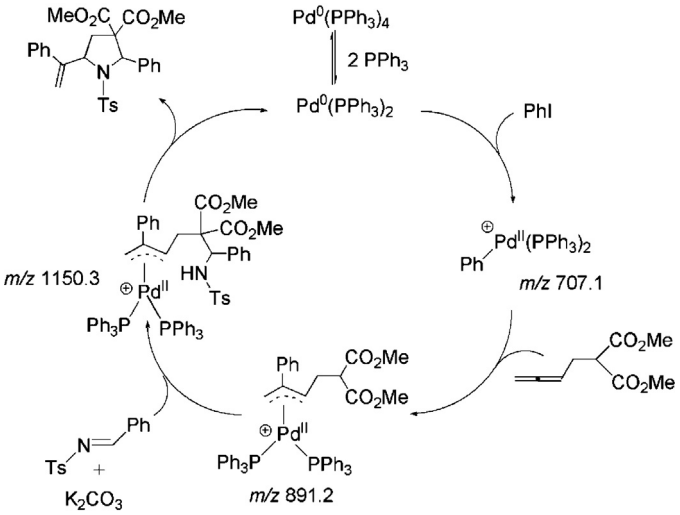

Scheme 12. Proposed mechanism for the formation of cis-pyrolidine derivatives from imine, iodobenzene and 2-(2,3-allenyl)malonate by ESI(+)-FTMS, *m/z* values are given for observed cationic intermediates.
Modified from reference [66].

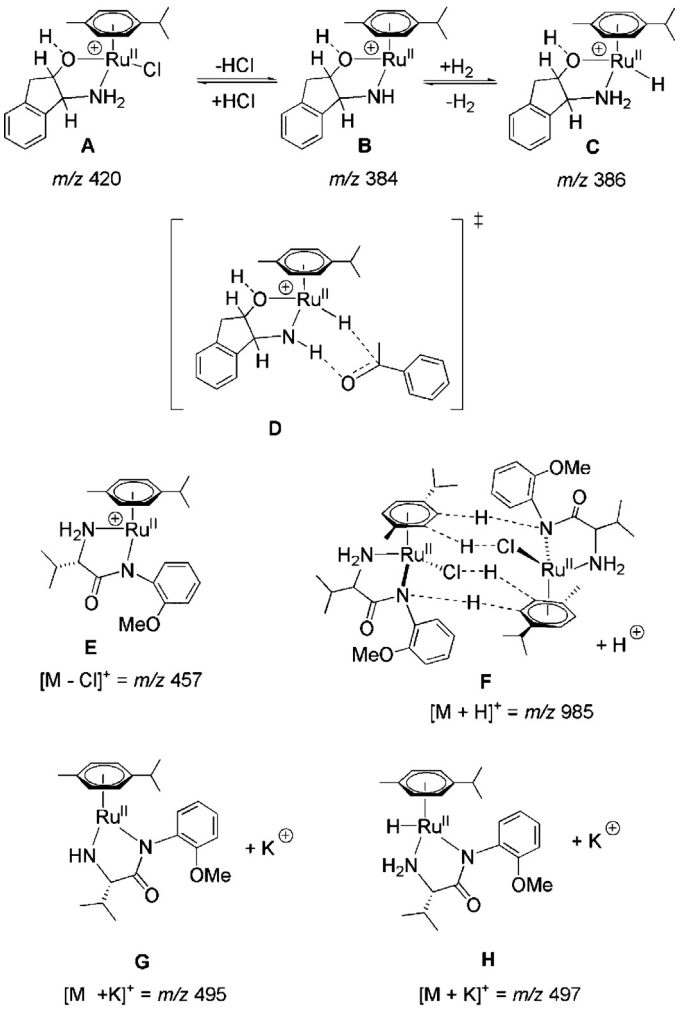

Fig. 10. Ruthenium-containing complexes observed by ESI(+)-MS.

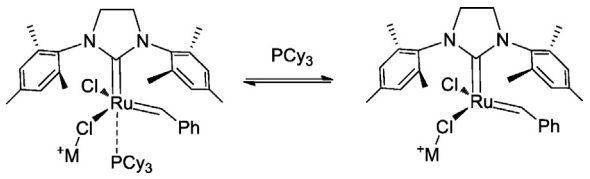

Scheme 13. Cationic Ru carbene complexes observed from solutions containing alkali metal chlorides. H_2IMes = 1,3-Bis(2,4,6-trimethylphenyl)-4,5-dihydroimidazol-2-ylidene, M = Li^+, Na^+, K^+, Cs^+ [73].

pre-catalyst $[Ru^{II}Cl(\eta^6\text{-cymene})]_2$ and *cis*-aminoindanol ($C_9H_{10}NO$) in isopropanol, in the absence of any substrate. Upon addition of acetophenone as a substrate no new peaks were observed [67]. The authors suggest that these results support the mechanism proposed by Noyori involving a six-centred transition state in which the substrate is not directly bound to the metal (Fig. 10D) [68].

A similar study employing both ionization modes examined the asymmetric hydrogenation of acetophenone, but with Ru^{II}-arene catalysts containing amino amide ligands: Ru(cymene)Cl(N–N) where N–N = $H_2NCH(^iPr)C(O)N((o\text{-}OMe)C_6H_4)$. Peaks were seen (by loss of Cl^- or gain of H^+ or K^+) corresponding to the monomer and piano stool-type dimers of the precatalyst, the 16-electron active catalyst, and a hydride-containing intermediate (Fig. 10E–H respectively). This provided further support for Noyori's mechanism and highlighted the potential involvement of dimers in the catalysis [10].

Ruthenium-based metathesis reactions have also been subject to a number of ESI-MS studies. We note that these systems have been studied extensively in the gas phase by Chen; however, this work is beyond the scope of our review. Chen also pioneered the study of these systems in the condensed-phase using a charge-tagged substrate (see Section 1.1.3) [69].

Metzger and his coworkers have investigated the solution-phase speciation of various ruthenium-based metathesis catalysts, and notably have used an in-line mixing tee to perpetually sample the reaction mixtures after just 12 s of mixing. Metzger used metallation by Li^+, Na^+, K^+, Cs^+ (in the form of their chloride salts) as an ionization technique to visualize the otherwise neutral catalysts in solution-phase metathesis reactions using first and second generation Grubbs catalysts [70]. This study was undertaken after they noted some disadvantages in using a charge-tagged phosphine to investigate the same system (see Section 1.1.3) [71]. In a later paper, the same metallation approach was used to investigate second-generation and Hoveyda–Grubbs olefin metathesis catalysts [72]. Both studies allowed the observation of the coordinatively unsaturated 14-electron active catalyst formed by dissociation of PCy_3 (Scheme 13). The authors propose that this activated species is in fact sampled directly from solution; however, they did not explicitly rule out the possibility that loss of a ligand occurred during the ESI process. In a number of cases the typically neutral catalysts were also observed by ESI-MS through electrochemical oxidation during the ESI process or through loss of a chloride. In both

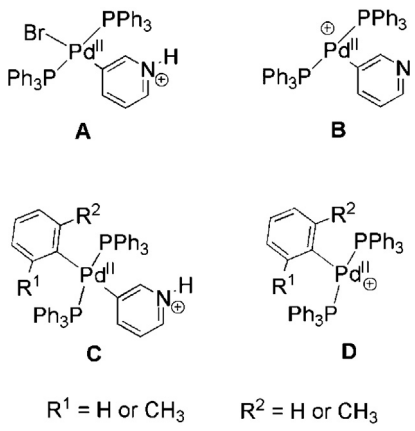

Fig. 11. (A and B) Oxidative addition intermediates $[(pyrH)Pd(PPh_3)_2Br]^+$ and $[(pyr)Pd(PPh_3)_2]^+$, (C & D) Transmetallation intermediates $[(pyrH)(R_1R_2C_6H_3)Pd(PPh_3)_2]^+$ and $[(R_1R_2C_6H_3)Pd(PPh_3)_2]^+$ (R_1 = H or CH_3 and R_2 = H or CH_3).

metallation-based studies the effects and role of the alkali metals were investigated with the help of theoretical calculations. Most recently, in 2013, the metallation approach was used by Binder et al. to compare the activities of the first and the third generation Grubbs catalysts. MS analysis revealed a substantial amount of unreacted catalyst species and not many oligomeric species in the first generation Grubbs while mostly oligomeric species were observed in the third generation Grubbs catalyst: in agreement with the high efficiency of the third generation catalysts [73].

4. Charged or chargeable tags

Interrogating catalytic reactions that have intrinsically- or adventitiously-charged intermediates is relatively straightforward, and analyses of these types of systems constitute the bulk of the literature on ESI-MS analysis of catalytic reaction mixtures, but many of the most important catalytic organometallic reactions proceed through neutral intermediates where there are no reliable ionization mechanisms for visualization by MS. In order to study these systems a charged or chargeable (usually having an acidic or basic site) tag is required. Importantly, the tag must not introduce steric or electronic effects that interfere with the catalysis in any significant way. Using a permanently charged tag has the additional benefit of generally improving signal intensity over chargeable systems, and it also guarantees that the tag will remain charged in solution despite changing reaction conditions. However, chargeable systems arguably provide greater flexibility in experiment design and may minimize any effect that the charge tag has on the reactivity of the species of interest. When introducing a charged tag it is also important to consider the potential influence of the counter-ion. Ideally the counter-ion should be non-coordinating (to avoid any interference at the metal centre) and have a low affinity for forming tight ion pairs with the charged tag (this will

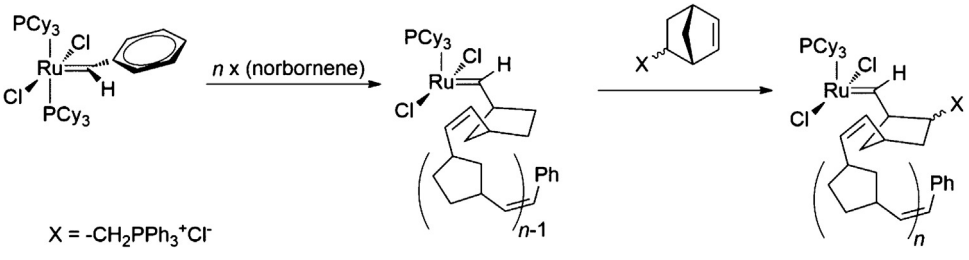

Fig. 12. Cationic norbornene as a charged-tag for detection by ESI-MS of ruthenium species involved in ring-opening metathesis polymerization [69].

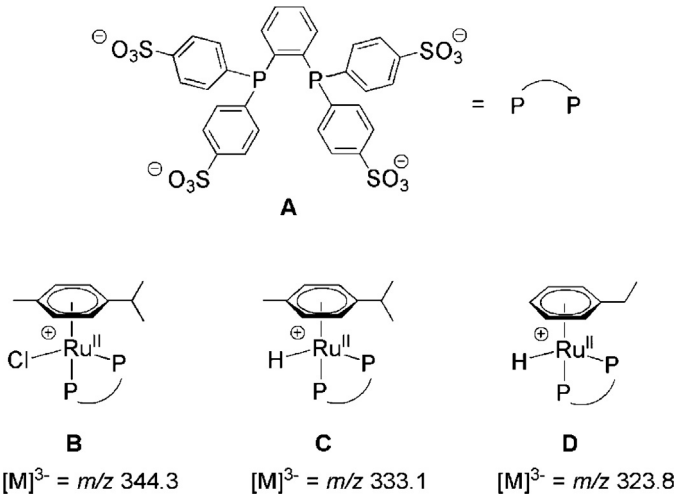

Fig. 13. Ruthenium species bearing a multiply-charged bidentate phosphine ligand and involved in the catalytic hydrogenation of styrene. Ions were detected in the negative-ion mode [11].

limit the formation of ion clusters and improve the electrospray performance of the charged tag by leaving the charged tag relatively exposed and electrospray-active). In practice, these aims can be readily achieved by using bulky non-coordinating ions – like $Ph_3P{=}N^+{=}PPh_3$ or PF_6^- – which can also help by improving the solubility of the charged tag in commonly used organic solvents.

In 1994, Canary et al. purposefully used a substrate with an easily protonated site to study the palladium-catalyzed reactions of pyridyl bromide with three different phenylboronic acids by ESI-MS. Pyridyl bromide was selected as a chargeable tag due to the ability of the ring nitrogen to become protonated. Relying on this ionization mechanism, oxidative addition intermediates and transmetallation intermediates were observed (Fig. 11) [74]. Since then, a majority of the existing reports are focused on the study of ruthenium-catalyzed systems, and they often make use of permanently-charged ligands that were initially designed to improve the water solubility of various catalysts. The groups of Traeger [75,76], Dyson [77], Nicholson [78] and Chen [79–81] have made significant contributions to this area; however, it is still a somewhat underappreciated approach.

Chen initiated the study of ruthenium-catalyzed reactions in solution in 2000 by doping a charged norbornene derivative into a solution containing catalyst and normal norbornene (Fig. 12). Initially the ruthenium catalyst is neutral and invisible by ESI-MS but as the norbornene monomers are incorporated, the mass spectrum shows a series of resting states of the catalyst after *n* additions of the monomer.

An investigation of the hydrogenation of styrene by Ru(II)-arene type catalysts with negatively-charged, water soluble, diphosphine ligands (Fig. 13A) was reported in 2004. Analysis by ESI(-)-MS

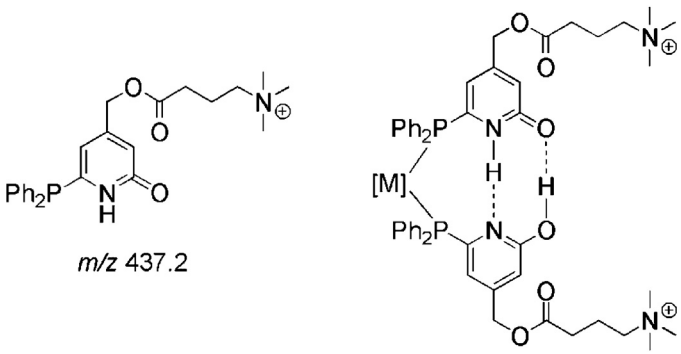

Fig. 15. A permanently-charged, self-assembling bidentate ligand for observation of metal catalysts by ESI(+)-MS [84].

yielded peaks corresponding to the anions $[Ru(\eta^2\text{-P-P})(\eta^6 p\text{-cymene})Cl]^{3-}$ (Fig. 13B), $[Ru(\eta^2\text{-P-P})(\eta^6 p\text{-cymene})H]^{3-}$ (Fig. 13C), and $[Ru(\eta^2\text{-P-P})(\eta^6\text{-PhC}_2H_5)H]^{3-}$ (Fig. 13D) and reveal an arene exchange process that is active during catalysis [11]. Further experiments demonstrated that the arene exchange process is only active in the presence of both substrate and dihydrogen and is not active when starting with the pre-formed hydride complex, all of which suggests that the exchange takes place on a dihydrogen-containing complex. H/D exchange experiments were also performed by ESI-MS and NMR and they demonstrate the presence of a dynamic equilibrium between a dihydrogen and hydride complex.

Two first generation ruthenium olefin metathesis catalysts were studied by Metzger [71] with the aid of the charged ligand $[P(Cy)_2(CH_2CH_2N(Me)_3)]^+\ Cl^-$, originally developed by Grubbs [82,83] as a water-soluble ligand (Fig. 14A and B). Inclusion of the charged ligand allowed ESI-MS observation of the proposed 14-electron catalytically-active Ru species (Fig. 14C), and confirmed many other aspects of the catalytic ring-closing metathesis cycle proposed by Grubbs. However, the authors noted in a subsequent paper that this methodology had the disadvantage that it could not be extended to second generation or Hoveyda–Grubbs catalyst, and that addition of excess phosphine may perturb the reaction.

Ruthenium-catalyzed hydroformylation of alkenes was also studied using charged tags [84]. A unique permanently-charged version of a self-assembling bidentate ligand (Fig. 15) was synthesized to study the catalytic mechanism.

Along with studies of the catalyst solution and stoichiometric reaction mixtures, the hydroformylation reaction was studied online under typical reaction conditions by connecting a pressurized autoclave (20 bar) directly to the mass spectrometer via a splitter. While this allowed them to identify new reaction intermediates they did not extract any kinetic data from the observed intermediates over time. Nevertheless, a new hydroformylation reaction mechanism for self-assembling ligands (in which the ligands play an active role in H_2 activation) was considered based on

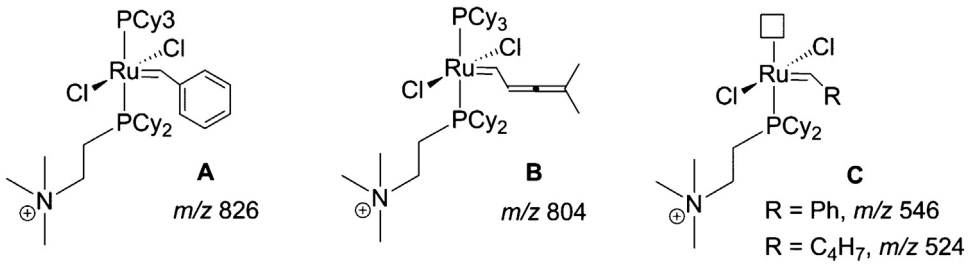

Fig. 14. Two charge-tagged analogues of first generation ruthenium olefin metathesis catalysts (A and B), and the corresponding 14-electron active species observed by ESI(+)-MS (C) [71].

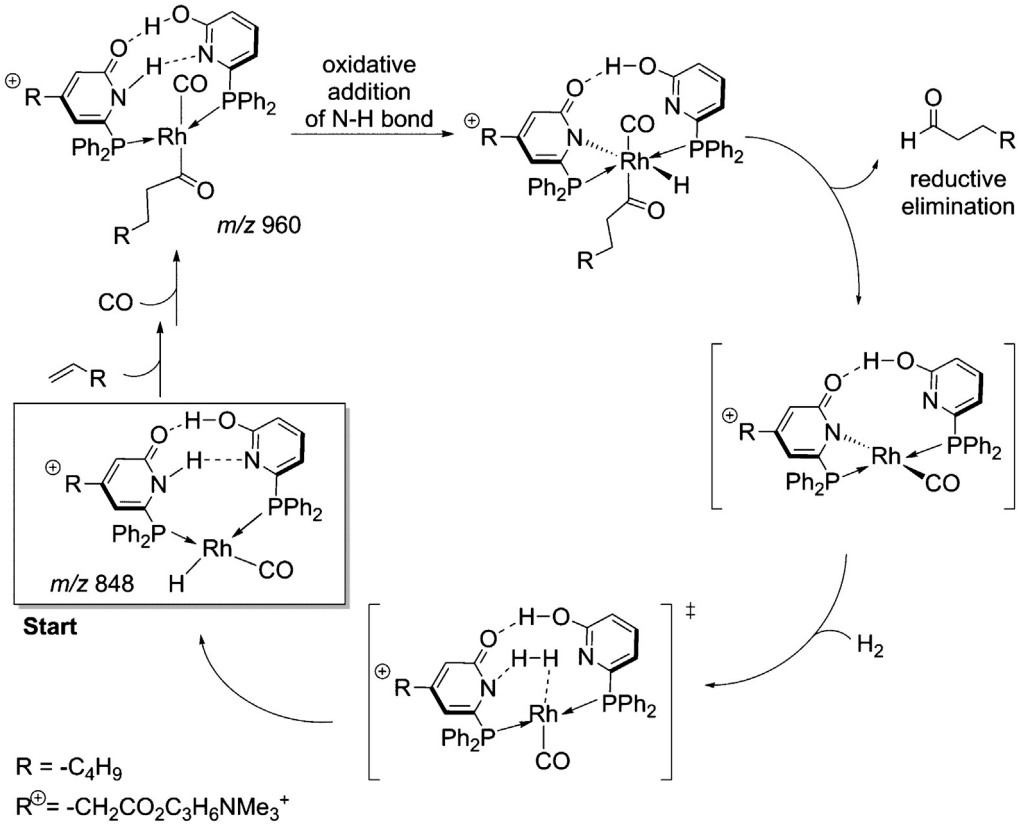

Scheme 14. A proposed ruthenium-catalyzed hydroformylation mechanism involving self-assembling ligands and informed by ESI(+)-MS analysis. Modified from reference [84].

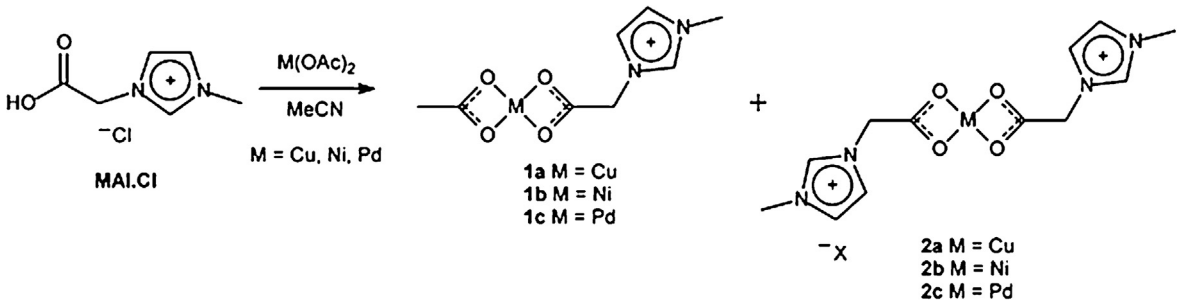

Scheme 15. Observation of charge-tagged complexes generated in reaction of charged-tagged acetylene imidazolium salt with neutral $M(OAc)_2$ complexes (M = Cu, Ni, Pd) [85].

their ESI-MS studies which included D_2-incorporation experiments (Scheme 14).

Eberlin has reported a charge-tagged acetate ligand as a probe for mass spectrometry [85]. Nickel, copper, and palladium complexes of this ligand have been synthesized and characterized by ESI-MS (Scheme 15). Also, catalytic activity of a charged-tagged acetylene imidazolium salt coordinated to Pd was examined in phosphine-free Heck and Suzuki cross coupling reactions. Greater activity and yield in comparison with $Pd(OAc)_2$ precatalyst along with ability to visualize neutral species in the reaction mixture indicate the dual role of this anionic ligand. Gas-phase reactivity of the metal complexes was also examined by CID from which rich

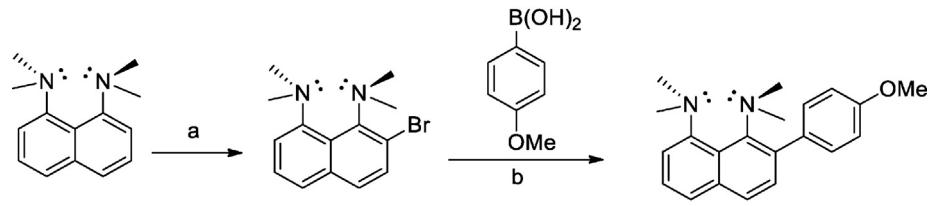

Scheme 16. Synthesis of 1,8-bis(dimethylamino)-2-(4-methoxyphenyl)naphthalene from proton sponge (1,8-bis(dimethylamino)naphthalene. (a) *N*-bromosuccinimide, THF and −78 °C. (b) $Pd(OAc)_2$, PPh_3, $NaCO_3H$ and mixture of *n*-propanol with water. Reflux 12 h [92].

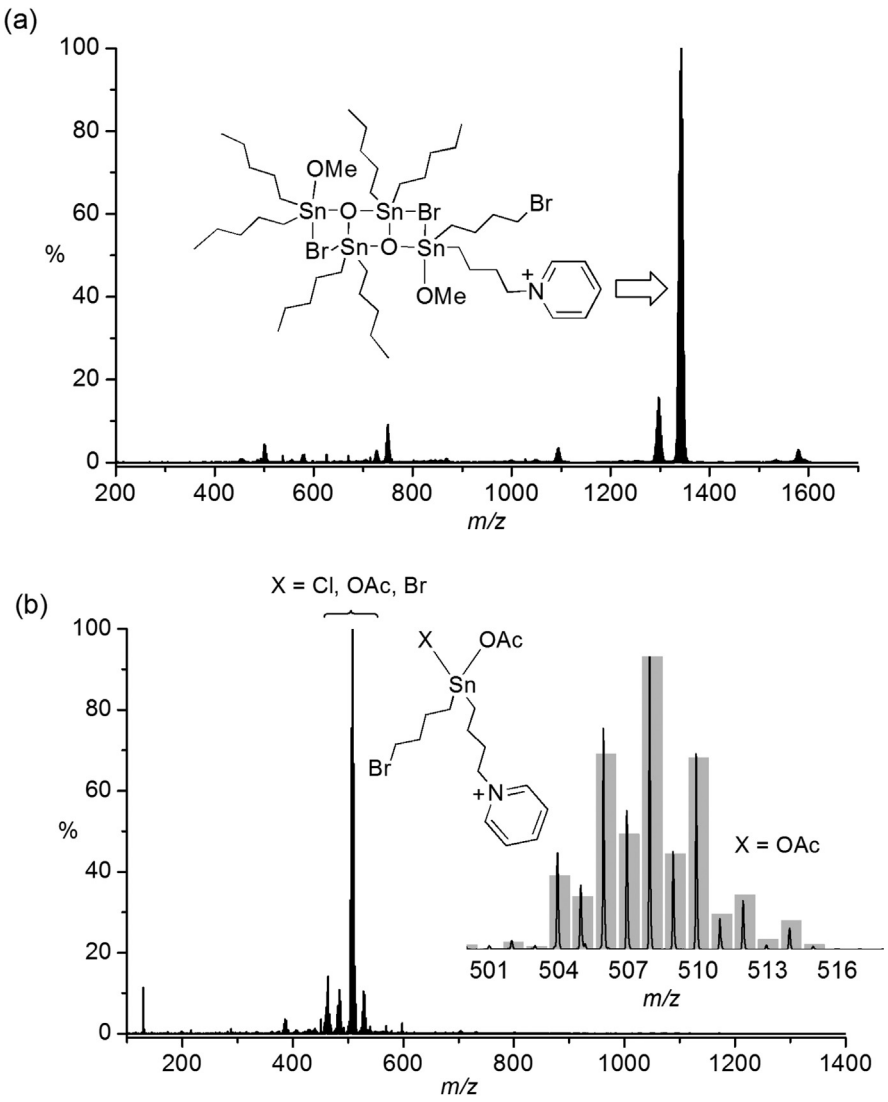

Fig. 16. (a) ESI(+)-MS of $[SnBrX(C_4H_8Br)(C_4H_8NC_5H_5)]^+$ Br^- (X = Cl or Br) with Bu_2SnO in methanol after 3 h reflux, (b) ESI(+)-MS of the reaction of $[SnBrX(C_4H_8Br)(C_4H_8NC_5H_5)]^+$ Br^- (X = Cl or Br) with Bu_2SnO in methanol after addition of acetic acid. Note the absence of any higher mass species in the presence of acid.

Modified figures from reference [90].

structural and reactivity information were obtained. Their findings explain some general mechanistic findings in palladium cross coupling reactions.

A palladium-catalyzed system in which charged tags were used was recently reported by Schade et al. This study also includes examples of the use of charged quaternary ammonium-tagged substrates for studying Zn, Mg and In systems by ESI-MS and described some true reaction-monitoring experiments (vide infra) [86].

Our group's contributions to the area of developing and employing charged and chargeable ESI-MS tags include: the development of various chargeable or charged phosphine ligands analogous to commonly used mono- or bi-dentate neutral phosphine ligands [87–89]; using a tethered charged pyridinium group to study distannoxane speciation during esterification catalysis [90]; and examining olefin hydrogenation and silane dehydrocoupling with a charged analogue of Wilkinson's catalyst [88,89].

A key example of the usefulness of charged tags in probing reaction mechanisms is found in our study of the esterification of alcohols and carboxylic acids [90] reportedly catalyzed by distannoxanes [91]. A permanently-charged pyridinium group was incorporated into the proposed distannoxane catalyst and the catalyst was then readily observed by ESI(+)-MS in solutions of methanol and acetonitrile (Fig. 16a). However, on addition of the carboxylic acid all distannoxane species (which are the proposed active catalysts) disappeared and instead mono-tin species dominated the spectra (Fig. 16b). This led to a number of control experiments in which the reaction was repeated in the presence of only mono-tin species and in the absence of all tin species with only HBr present (a byproduct formed on reaction of the carboxylic acid with the distannoxane). Surprisingly, the reaction proceeded most efficiently when only HBr was present suggesting that distannoxanes are in fact not the species responsible for catalyzing the esterification reaction.

Our group also recently reported a coordinating proton sponge ligand with a chargeable tag for analysis by ESI-MS. It was shown that the tag 1,8-bis(dimethylamino)-2-(4-methoxyphenyl)naphthalene (Scheme 16) has the characteristics of a practical chargeable tag for analysis by ESI-MS [92]. For example, the ligand readily coordinates to chromium in an η^6-fashion (Fig. 17) while the proton sponge moiety scavenges a proton from

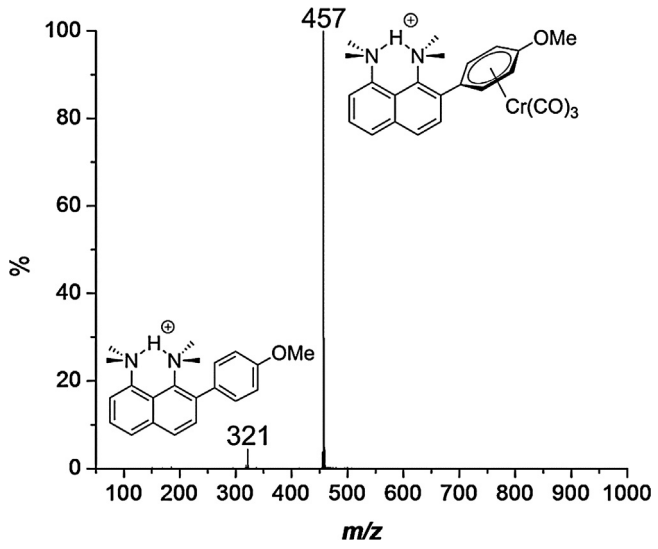

Fig. 17. ESI(+)-MS of the charge tagged chromium tricarbonyl complex in methanol (*m/z* 457). A small amount of free ligand is also observed (*m/z* 321).

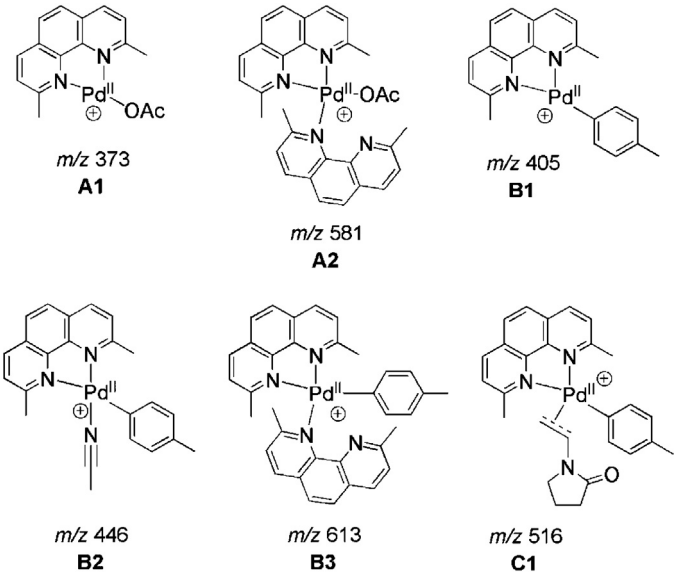

Fig. 19. Cationic intermediates in the oxidative Heck arylation of 1-vinyl-2-pyrrolidinone by *p*-tolylboronic acid observed by ESI(+)-MS [18].

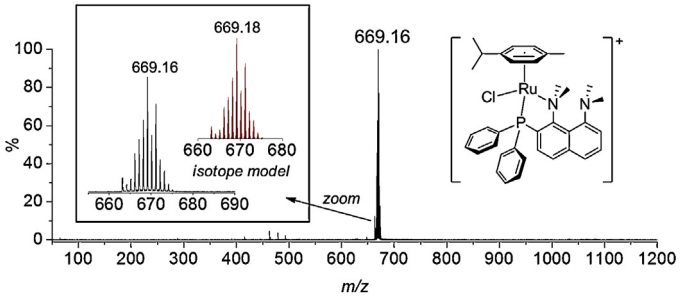

Fig. 18. ESI(+)-MS (top) of $[Ru(\eta^6\text{-}p\text{-cymene})Cl(C_{26}H_{27}N_2P)]^+$. MS/MS exhibited loss of *p*-cymene, suggesting that the phosphine is strongly bound and thus not monodentate [93].

solution to become charged with high efficiency. The large distance between the tag and active site ensures the innocent role of the tag on the reactivity of complex.

Care must be taken in designing chargeable tags since the acidic or basic site can also act in some cases as a metal-binding site, thus changing the normal reactivity of the catalyst. For example, 1,8-bis(dimethylamino)-2-diphenylphosphonaphthalene, Proton Sponge® substituted in the *ortho*-position by $-PPh_2$, exhibits non-innocent behaviour. Once the phosphine moiety binds to a metal (in this case ruthenium) the dimethylamino group is positioned to bind to the metal creating a 1,4-bidentate ligand (Fig. 18). MS/MS experiment on the complex $[Ru(\eta^6\text{-}p\text{-cymene})Cl(C_{26}H_{27}N_2P)]^+$ gave evidence of a strong N-Ru bond (Fig. 18). Appending phosphane in the 4-position of the naphthalene ring avoids this interference [93].

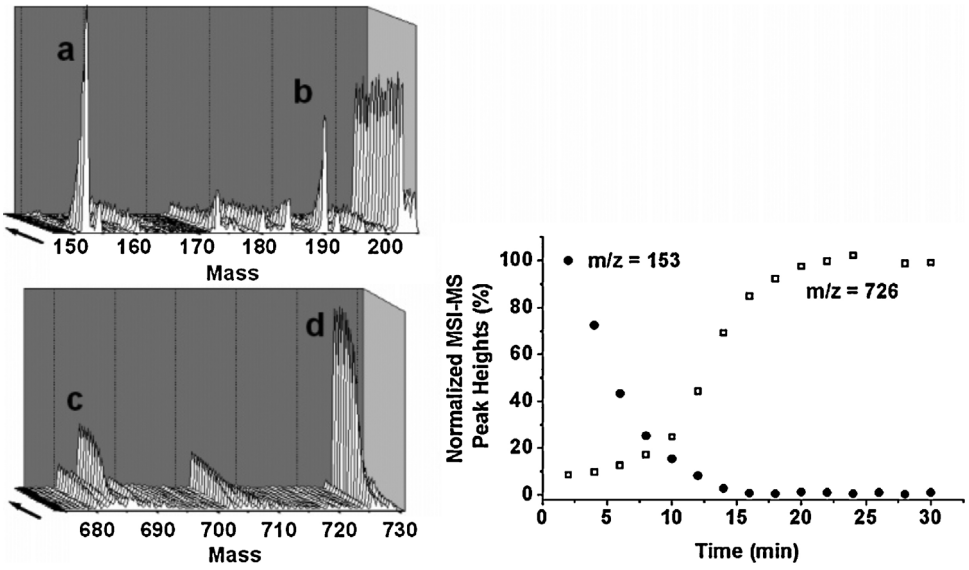

Fig. 20. (left) ESI(+)-MS of the catalytic solution showing spectra of two separate runs from 2 to 30 min (arrows represent the increase of time), with 2-min intervals. Assigned peaks are (a) *m/z* 153, $KH_2SO_5^+$, (b) *m/z* 191, $K_2HSO_5^+$, (c) *m/z* 684, $O_2(terpy)_2(OAc)(OH)]^+$, and (d) *m/z* 726, $[Mn^{III/IV}{}_2O_2(terpy)_2(OAc)_2]^+$. (right) Peak heights of *m/z* 153 and 726 over time.

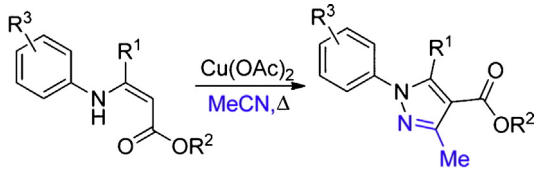

Scheme 17. Copper promoted synthesis of pyrazoles from enaminones [96].

5. Continuous reaction monitoring

Most of the experiments discussed above involve the sampling of metal-catalyzed reactions at discreet time intervals in order to assess the composition of the reaction mixture as the reaction progresses. While ESI-MS analysis of this type can reveal the presence of any low-concentration potential intermediates, simple detection of a low concentration species does not clarify its role in the overall solution phase reaction. In order to understand the role of observed species it would be highly desirable to monitor the reaction profile of key species continuously over the course of the reaction in such a way that kinetic data can be obtained [8,18,86,89]. A few groups, including our own, have worked to develop such methodology. Here we will briefly discuss the origins of this methodology and describe recent work in the area from our group. A related micro-review [94] and book [95] by Santos discusses online ESI-MS investigations of primarily organo-catalyzed reactions but also includes some organometallic examples.

A precursor to continuous monitoring studies was reported in 2006 by Enquist in which an oxidative Heck-type reaction was sampled periodically and a graph of the intensities of all the observed intermediates was generated. In Fig. 19 cationic palladium complexes are shown which were directly observed by ESI-MS and correspond to the active catalyst (A1 and A2), transmetallated intermediates (B1–B3), and a palladium-bound olefin intermediate (C1) [18]. By examining the intensity of these intermediates over time the investigators noticed that intermediates corresponding to the catalyst at the beginning of the cycle (Fig. 19A1 and A2) increased throughout the reaction while the intensity of intermediates related to transmetallation (Fig. 19B1–B3) decreased. From this they postulated that the rate of the transmetallation step decreased over time as the transmetallation partner (an arylboronic acid) was consumed.

Reaction monitoring by ESI-MS is not limited to monitoring catalytic intermediates, valuable information can also be obtained by monitoring the interplay of the various reactants in solution. In 2007, a manganese-catalyzed oxygen-evolving system that acts as a model for the oxygen-evolving complex of photosystem II was also studied by periodic sampling and analysis by ESI-MS (as well as EPR, UV/Vis, and XAS). The highly oxidized dinuclear complex $Mn^{III/IV}{}_2O_2(terpy)_2(SO_4)_2$ was determined to be the dominant species in solution but an observed correlation over time in the ESI mass spectra between $[Mn^{III/IV}{}_2O_2(terpy)_2(OAc)_2]^+$ (m/z 726) and the oxidant $[KH_2SO_5]^+$ (m/z 153) led to the conclusion that the binuclear $Mn^{III/IV}$ species was in fact the active precatalyst (Fig. 20) [8]. The reaction solution was sampled by ESI-MS approximately every 2.5 min.

Since ESI-MS analysis provides data on all charged species in the reaction mixture over the course of a reaction it is also possible to use ESI-MS monitoring to uncover entirely unexpected intermediates, co-catalysts or side products in a reaction. This was the case in a study of the copper-catalyzed synthesis of pyrazoles in the presence of CH_3CN which involves C—C and N—N bond formation of an enaminone (Scheme 17).

An unknown copper-containing complex, $[(\mathbf{X})Cu]^+$, was observed which had the kinetic profile of a potential intermediate (see Fig. 21). Based the initial detection by ESI-MS compound **X** was isolated and structurally characterized by multidimensional NMR spectroscopy as an imidazolid-3-one derivative. Reactivity studies on the isolated compound **X** suggested that **X** was not a true intermediate but rather a side product [96]. Nevertheless, this work demonstrates the potential of reaction-monitoring by ESI-MS to provide substantial mechanistic insights.

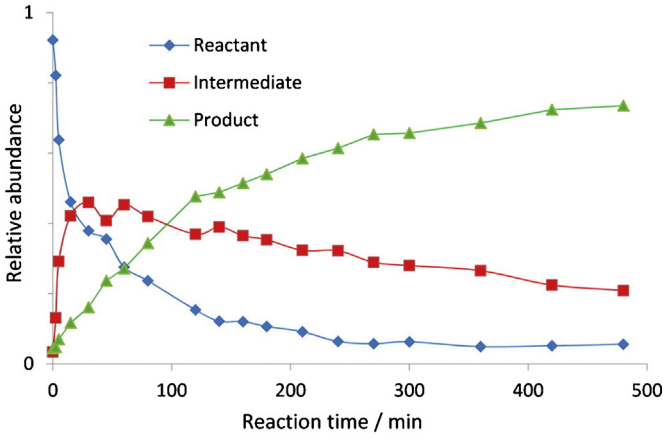

Fig. 21. Relative intensities of the main components of the reaction of methyl 3-(phenylamino)but-2-enoate in the presence of copper acetrate and acetonitrile at 110 °C as monitored by ESI-MS in the positive ion mode. The sum of ions representing the reactant, the product, and the potential intermediate ($[(\mathbf{X})Cu]^+ + [(\mathbf{X})Cu(CH_3CN)]^+$) are shown.

Reprinted with permission from "Electrospray Ionization Mass Spectrometry Reveals an Unexpected Coupling Product in the Copper-Promoted Synthesis of Pyrazoles" K. Jiang, G. Bian, Y. Chai, H. Yang, Q. Lai and Y. Pan, *Int. J. Mass Spectrom.* 2012, 321–322, 40–48. Copyright ©2013, American Chemical Society.

In 2010 the self-assembly of a hybrid polyoxometalate (POM) was studied by "real-time" monitoring of ESI-MS. A pathway was proposed based on observed intermediates followed by rearrangement of $[\alpha\text{-}Mo_8O_{26}]^{4-}$, coordination of Mn^{III} and coordination of two tris(hydroxymethyl)aminomethane ligands (TRIS) to form a symmetrical Mn cluster [97].

In 2010, a palladium-catalyzed Negishi cross-coupling reaction between the quaternary ammonium charged substrate (*p*-iodophenyl)-trimethyl-ammonium iodide ($[ArI]^+I^-$) and

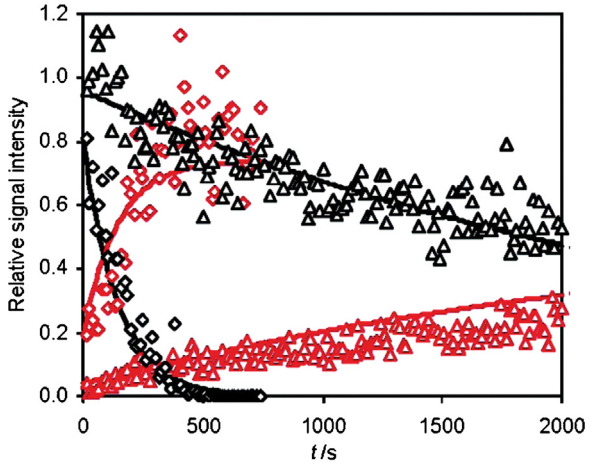

Fig. 22. Time dependence of the normalized signal intensities of reactant $[ArI]^+$ (m/z 262, black) and product $[ArBn]^+$ (m/z 226, red) formed in the Pd-catalyzed cross-coupling reaction with BnZnBr in CH_3CN at room temperature as determined by ESI mass spectrometry. Results of two experiments with different catalyst loadings are shown (diamond = 100 mol%, triangle = 5 mol% relative to $[ArI]^+$).

Reprinted with permission from [86]. Copyright ©2010 American Chemical Society. (For interpretation of the references to color in this figure legend, the reader is referred to the web version of the article.)

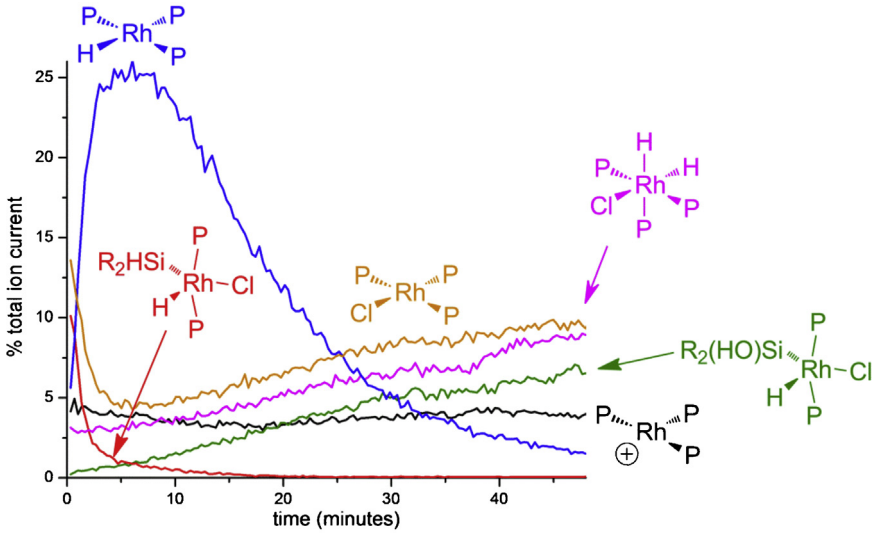

Fig. 23. Reaction profile of the six Rh-containing species observed over time by ESI-MS. Each trace is generated by normalizing of each species to the total ion current. Consumption of the RhP_3H species was approximately first order [89].

benzylzincbromide to form (*p*-benzylphenyl)-trimethyl-ammonium iodide ($[ArBn]^+I^-$) was monitored continuously using ESI-MS [86]. Reaction mixtures were drawn into a syringe and injected continuously at room temperature into the mass spectrometer over 30 min beginning approximately 2 min after the start of the reaction (Fig. 22). A plot of relative signal intensity versus time is obtained, and signals for the reactant and product are shown (the results for two different catalyst loadings are shown). The authors stated that the high noise levels are a result of the inherently poor signal stability of the ESI process. They were able to successfully observe the effects of catalyst loading and reagent concentration on the reaction, and derived a rate constant for the oxidative addition of (*p*-iodophenyl)-trimethyl-ammonium to palladium at room temperature ($k_2 = 4 \pm 2\ L\ mol^{-1}\ s^{-1}$).

The reaction of Wilkinson's catalyst with a dialkylsilane was examined using continuous monitoring ESI-MS and the charged phosphine ligand $[Ph_2P(CH_2)_4PPh_2(CH_2Ph)]^+[BF_4]^-$ as an ESI handle [89]. In contrast to the previous examples where only the kinetics of the reactant and products were observed, these experiments examined only reaction intermediates which contained the charged phosphine tag. This remains one of the greatest strengths of ESI-MS as a mechanistic tool – analysis of low-concentration intermediates directly from complex reaction mixtures is possible. Stoichiometric solutions of $RhCl(PPh_3)_3$ and $(n\text{-hexyl})_2SiH_2$ doped with the charged ligand were injected into the MS continuously directly from a syringe pump in an adjacent glovebox. The ESI-MS data confirmed the speciation of the reaction mixture that was observed by NMR experiments and a number of additional species were identified (Fig. 23). Behaviour of each observed complex over time allowed the proposal of a reaction mechanism for the dehydrocoupling of silane including a competing catalyst decomposition pathway that is present due to trace amounts of water.

Direct infusion of a reaction mixture from a syringe in to a mass spectrometer (as in the previous example) is only a viable sampling method for some of the simplest catalytic reactions. In order to take full advantage of continuous monitoring by ESI-MS one would ideally like to monitor catalytic systems under completely normal reaction conditions. This may include stirring, heating or cooling, and the maintenance of an inert atmosphere: all of which are difficult or impossible to replicate effectively within a syringe. Our group has developed the technique "pressurized sample infusion mass spectrometry" (PSI-MS) to address these requirements. PSI-MS allows the continuous collection of real-time kinetic data for reaction mixtures under standard reaction conditions by infusing a reaction mixture from a slightly pressurized reaction flask directly into the source of a mass spectrometer via a short length of PEEK tubing [98].

A recent example is the kinetic analysis of rhodium-catalyzed alkyne hydrogenation [99]. By employing the charge-tagged alkyne substrate, $[Ph_3P(CH_2)_4C_2H]^+[PF_6]^-$, continuous kinetic data can be gathered for the reactant, the alkene product and the alkane product. Excellent agreement of the experimental data with numerical modelling (Fig. 24) based on the well-established mechanism for this reaction verifies the suitability of PSI-MS as a method of collecting reliable kinetic data. Because the turnover-limiting step is dissociation of PPh_3 to generate the 14-electron $Rh(PPh_3)_2Cl$, addition of extra PPh_3 slows the reaction in a predictable way.

It is clear that the most useful data sets can be extracted from systems in which reactants, product and intermediates can be monitored *simultaneously* over the course of the reaction. In this way, a direct link can be made between the overall reaction progress and the kinetic profiles of the various reactive species. The mechanistic investigation of the copper-free Sonogashira reaction to form a new C—C bond between and aryl halide and a terminal alkyne is an example [100]. When the charged aryl iodide substrate $[p\text{-}IC_6H_4CH_2PPh_3]^+$ was doped into a typical catalytic reaction mixture, MS signals were observed for the reactant, product, byproduct and – at 100× magnification – the intermediates $[PdL_n(Ar)(I)]^+$ and $[PdL_n(Ar)(C_2Ph)]^+$. Based on the behaviour of the intermediates and the rate of formation of product under various reaction conditions it was deduced that a build-up of H^+ in solution over the course of the reaction impeded the formation of product. With this information a better set of reaction conditions was selected which involved the addition of a stronger base to more effectively sequester the generated H^+. The observed formation of a dehalogenated byproduct in the reaction was also investigated in detail by PSI-MS in similar fashion (Fig. 25), and unusually strong primary kinetic isotope effects were detected, suggesting an alternative mechanism at play under these conditions [101].

The Pauson–Khand reaction was studied in a similar manner [102]. A single intermediate was observed for the [2+2+1] intramolecular cycloaddition which corresponded to the charged piperidinium substrate coordinated to a hexacarbonyl dicobalt complex (Fig. 26). This observation along with large positive enthalpy and entropy of activation values (calculated from PSI-MS data) supported the theory that CO dissociation is the rate limiting

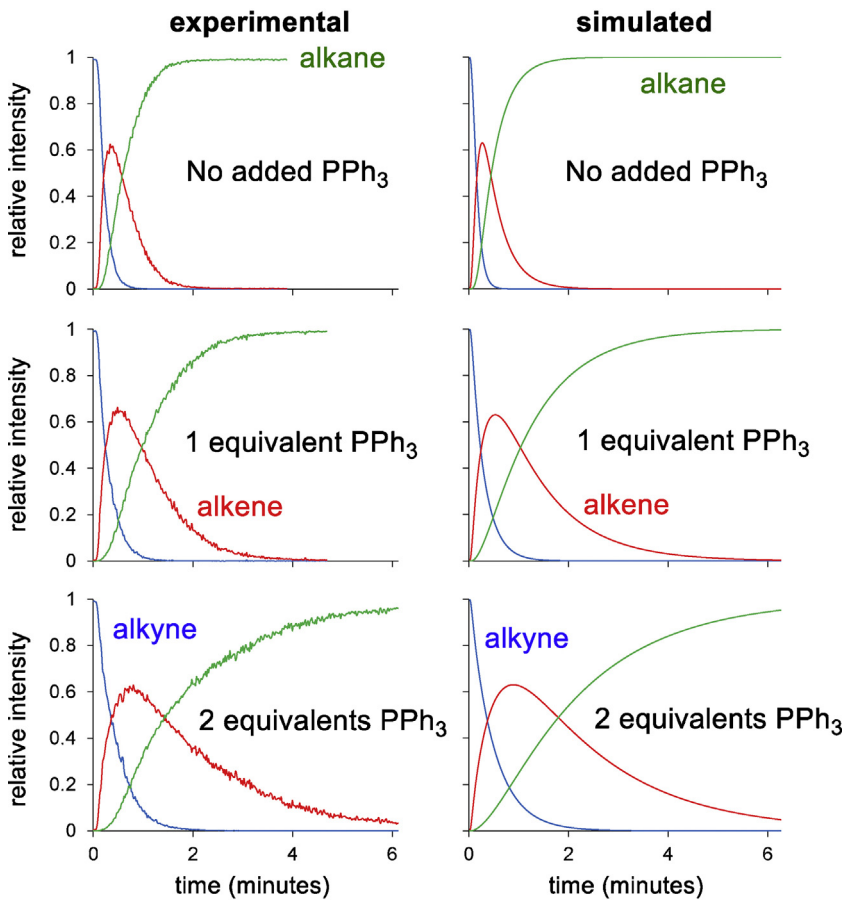

Fig. 24. Experimental (left) and calculated (right) traces for the relative intensities of reactant (blue), alkene product (red) and alkane product (green) over the course of a hydrogenation reaction catalyzed by Wilkinson's catalyst with varying initial amounts of excess triphenylphoshpine. (For interpretation of the references to color in this figure legend, the reader is referred to the web version of the article.)

step after which alkene coordination and CO incorporation occur quickly to give the final product.

Finally, the details of how an active catalyst is formed from the various ingredients that go into a reaction mixture are often overlooked. But understanding these processes can dramatically improve reaction efficiency and effectiveness. Once again, PSI-MS can provide an expedient way to examine these processes. The preparation of $[Pd(PPh_3)_2(Ar)(I)]$ from [Pd(tmeda)(Ar)(I)], tmeda = tetramethylethylenediamine was monitored in real time by PSI-MS using a charge-tagged aryl ligand ($-C_6H_4CH_2PPh_3^+ PF_6^-$) [103]. Contrary to the expected simple substitution of tmeda by two equivalents of triphenylphosphine, there was an initial fast substitution of iodide for triphenylphosphine followed by a much slower displacement of tmeda and re-coordination of iodide (Fig. 27).

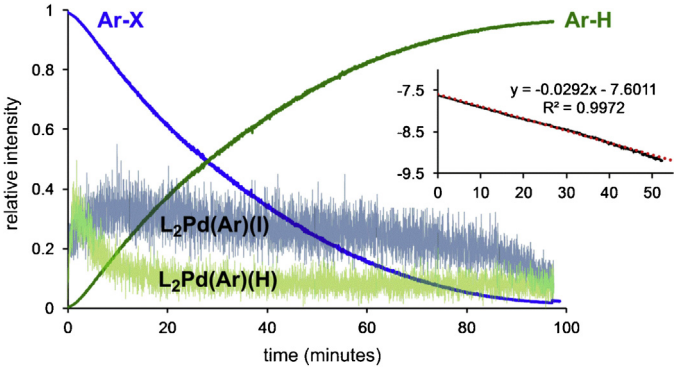

Fig. 25. Hydrodehalogenation progress observed by (+)-MS with intensities over time of all key species bearing the charged tag (Ar = $[C_6H_4CH_2PPh_3]^+$; L = PPh_3). The intensities of the palladium-containing intermediates have been multiplied by 100. Inset: plot demonstrating the first order kinetics.
Reprinted with permission from reference [101].

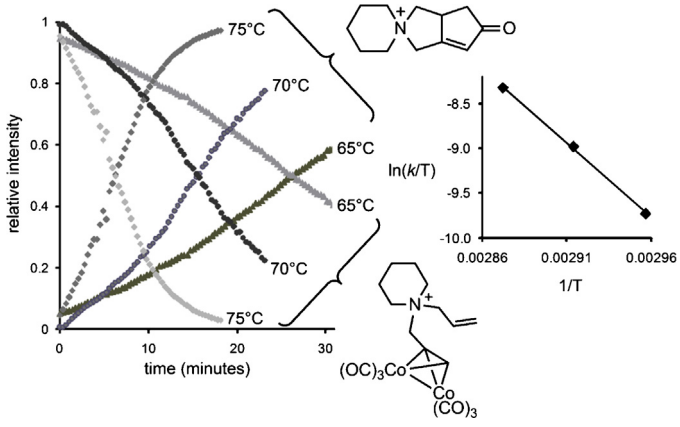

Fig. 26. Rate of formation of product from $[Co_2(CO)_6(ligand)]^+$ at 65, 70 and 75 °C. System was pressurized with CO gas and sample infused with online dilution with acetone to the source of ESI-MS.
Modified with permission from reference [102].

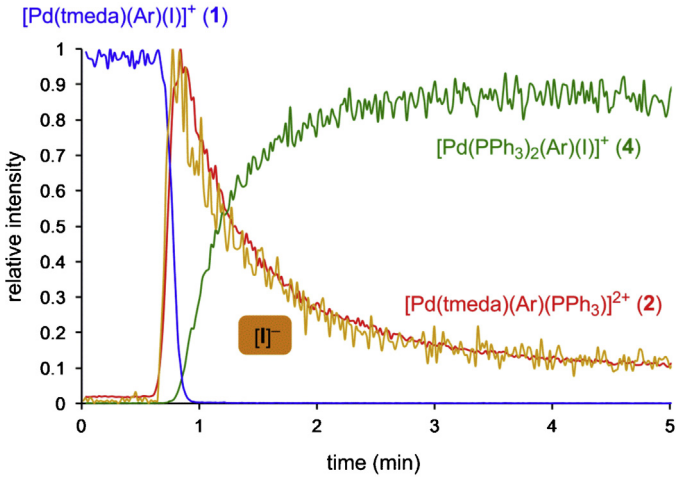

Fig. 27. PSI-MS monitoring of the reaction progress for the preparation of [Pd(PPh$_3$)$_2$(Ar)(I)] from [Pd(tmeda)(Ar)(I)]. The blue, red and green traces were collected in the positive ion mode and the orange trace was collected in the negative ion mode [103]. (For interpretation of the references to color in this figure legend, the reader is referred to the web version of the article.)

By monitoring the reaction in the negative ion mode as well as in the positive ion mode the appearance and disappearance of free iodide in solution can also be directly monitored and its kinetic profile perfectly coincides with the kinetics of the observed cationic metal complexes. This new understanding of how [Pd(PPh$_3$)$_2$(Ar)(I)] is generated allowed the development of a simple and general protocol for making different complexes of the type [Pd(PPh$_3$)$_2$(Ar)(X)] where X = Br, Cl and F.

6. Conclusions

We need robust and efficient catalysts to facilitate the synthesis of next-generation materials, pharmaceuticals and commodity chemicals. As a result it is increasingly important that we understand the detailed workings of homogeneous catalytic reactions. ESI-MS is a promising mechanistic tool for understanding complex and dynamic solution-phase reactions.

The field has experienced rapid growth stemming from the introduction of ESI-MS as an ionization method which can gently transfer solution-phase ions into the gas phase. In some cases the species of interest in a catalytic reaction are already charged in solution (or can easily become charged), and are thus easily analyzed by ESI-MS. But in cases where the reactants, products or potential intermediates are un-charged the use of charged or chargeable tags – which can be covalently attached to a ligand or one of the reactants – allows for analysis by ESI-MS. With charged-tags in hand, investigations of catalytic organometallic reactions by ESI-MS have become increasingly sophisticated over the last decade: moving from simple identification of potential catalytic intermediates from a reaction mixture to the real-time collection of continuous kinetic data for reactants, products and intermediates simultaneously under standard reaction conditions.

Looking ahead, it seems clear that approaches that partner multiple techniques together will be needed for a complete picture of the reacting mixture. All methods of analysis have their advantages and disadvantages, and ESI-MS is no exception; most progress will be made when synergistic combinations are devised that harness the strengths of the techniques (in the case of ESI-MS, speed, sensitivity and the capability to study complex mixtures) and minimize their weaknesses (for ESI-MS, a huge blind spot with respect to uncharged molecules).

Acknowledgements

JSM thanks NSERC (Discovery and Discovery Accelerator Supplement) for operating funds, and CFI, BCKDF and the University of Victoria for infrastructural support.

References

[1] J.F. De la Mora, G.J. Van Berkel, C.G. Enke, R.B. Cole, M. Martinez-Sanchez, J.B. Fenn, J. Mass Spectrom. 35 (2000) 939–952.
[2] M.N. Eberlin, Eur. J. Mass Spectrom. 13 (2007) 19–28.
[3] K.W.M. Siu, R. Guevremont, J.C.Y. Le Blanc, G.J. Gardner, S.S. Berman, J. Chromatogr. 554 (1991) 27–38.
[4] A.J. Canty, P.R. Traill, R. Colton, I.M. Thomas, Inorg. Chim. Acta 210 (1993) 91–97.
[5] M. Bonchio, G. Licini, G. Modena, O. Bortolini, S. Moro, W.A. Nugent, J. Am. Chem. Soc. 121 (1999) 6258–6268.
[6] Z. Li, Z.H. Tang, X.X. Hu, C.G. Xia, Chem. Eur. J. 11 (2005) 1210–1216.
[7] B.C. Gilbert, J.R. Lindsay Smith, A. Mairata i Payeras, J. Oakes, R. Pons i Prats, J. Mol. Catal. A: Chem. 219 (2004) 265–272.
[8] H. Chen, R. Tagore, G. Olack, J.S. Vrettos, T.-C. Weng, J. Penner-Hahn, R.H. Crabtree, G.W. Brudvig, Inorg. Chem. 46 (2007) 34–43.
[9] P.J. Dyson, K. Russell, T. Welton, Inorg. Chem. Commun. 4 (2001) 571–573.
[10] P. Pelagatti, M. Carcelli, F. Calbiani, C. Cassi, L. Elviri, C. Pelizzi, U. Rizzotti, D. Rogolino, Organometallics 24 (2005) 5836–5844.
[11] C. Daguenet, R. Scopelliti, P.J. Dyson, Organometallics 23 (2004) 4849–4857.
[12] C. Vicent, M. Viciano, E. Mas-Marza, M. Sanau, E. Peris, Organometallics 25 (2006) 3713–3720.
[13] S.R. Wilson, Y. Wu, Organometallics 12 (1993) 1478–1480.
[14] C. Raminelli, M.H.G. Prechtl, L.S. Santos, M.N. Eberlin, J.V. Comasseto, Organometallics 23 (2004) 3990–3996.
[15] C. Chevrin, J. Le Bras, F. Henin, J. Muzart, A. Pla-Quintana, A. Roglans, R. Pleixats, Organometallics 23 (2004) 4796–4799.
[16] J. Masllorens, I. Gonzalez, A. Roglans, Eur. J. Org. Chem. (2007) 158–166.
[17] A.A. Sabino, A.H.L. Machado, C.R.D. Correia, M.N. Eberlin, Angew. Chem., Int. Ed. 43 (2004) 2514–2518.
[18] P.A. Enquist, P. Nilsson, P. Sjoberg, M. Larhed, J. Org. Chem. 71 (2006) 8779–8786.
[19] A. Svennebring, P.J.R. Sjoberg, M. Larhed, P. Nilsson, Tetrahedron 64 (2008) 1808–1812.
[20] C. Chevrin, J. Le Bras, A. Roglans, D. Harakat, J. Muzart, New J. Chem. 31 (2007) 121–126.
[21] C. Markert, M. Neuburger, K. Kulicke, M. Meuwly, A. Pfaltz, Angew. Chem., Int. Ed. Engl. 46 (2007) 5892–5895.
[22] A. Roglans, A. Pla-Quintana, in: L.S. Santos (Ed.), Reactive Intermediates: MS Investigations in Solution, Wiley-VCH Verlag GmbH & Co. KGaA, Weinheim, 2010, pp. 229–275.
[23] R.A.J. O'Hair, in: L.S. Santos (Ed.), Reactive Intermediates: MS Investigations in Solution, Wiley-VCH Verlag GmbH & Co. KGaA, Weinheim, 2010, pp. 199–227.
[24] J.S. McIndoe, in: R.D. Jack Yarwood, Simon Duckett (Eds.), Spectroscopic Properties of Inorganic and Organometallic Compounds, Royal Society of Chemistry, Cambridge, 2010, pp. 288–308.
[25] J.C. Traeger, Int. J. Mass Spectrom. 200 (2000) 387–401.
[26] D.A. Plattner, Int. J. Mass Spectrom. 207 (2001) 125–144.
[27] R. Jirásko, M. Holčapek, Mass Spectrom. Rev. 30 (2011) 1013–1036.
[28] D. Agrawal, D. Schröder, Organometallics 30 (2011) 32–35.
[29] J. Roithova, Chem. Soc. Rev. 41 (2012) 547–559.
[30] M. Bonchio, O. Bortolini, V. Conte, S. Primon, J. Chem. Soc. Perkin Trans. 2 (2001) 763–765.
[31] M. Bonchio, G. Licini, G. Modena, S. Moro, O. Bortolini, P. Traldi, W. Nugent, Chem. Commun. (Cambridge) (1997) 869–870.
[32] O. Bortolini, M. Carraro, V. Conte, S. Moro, Eur. J. Inorg. Chem. 2003 (2003) 42–46.
[33] B.C. Gilbert, N.W.J. Kamp, J.R. Lindsay Smith, J. Oakes, J. Chem. Soc. Perkin Trans. 2 (1998) 1841–1844.
[34] B.C. Gilbert, J.R. Lindsay Smith, M.S. Newton, J. Oakes, R. Pons i Prats, Org. Biomol. Chem. 1 (2003) 1568–1577.
[35] C. Kim, K. Chen, J. Kim, L. Que Jr., J. Am. Chem. Soc. 119 (1997) 5964–5965.
[36] D. Feichtinger, D.A. Plattner, Angew. Chem., Int. Ed. Engl. 36 (1997) 1718–1719.
[37] Z.O. Oyman, W. Ming, R. Van der Linde, Appl. Catal. A 316 (2007) 191–196.
[38] L. Dubois, R. Caspar, L. Jacquamet, P.-E. Petit, M.-F. Charlot, C. Baffert, M.-N. Collomb, A. Deronzier, J.-M. Latour, Inorg. Chem. 42 (2003) 4817–4827.
[39] L. Dubois, D.-F. Xiang, X.-S. Tan, J.-M. Latour, Eur. J. Inorg. Chem. 2005 (2005) 1565–1571.
[40] J.A. Lessa, A. Horn, E.S. Bull, M.R. Rocha, M. Benassi, R.R. Catharino, M.N. Eberlin, A. Casellato, C.J. Noble, G.R. Hanson, G. Schenk, G.C. Silva, O.A.C. Antunes, C. Fernandes, Inorg. Chem. 48 (2009) 4569–4579.
[41] C.-X. Yin, R.G. Finke, J. Am. Chem. Soc. 127 (2005) 9003–9013.
[42] A. Fujii, E. Hagiwara, M. Sodeoka, J. Am. Chem. Soc. 121 (1999) 5450–5458.
[43] Y.-H. Gao, L. Yang, W. Zhou, L.-W. Xu, C.-G. Xia, Appl. Organomet. Chem. 23 (2009) 114–118.
[44] K. Kikukawa, T. Matsuda, Chem. Lett. 6 (1977) 159–162.

[45] H.A. Stefani, J.M. Pena, K. Gueogjian, N. Petragnani, B.G. Vaz, M.N. Eberlin, Tetrahedron Lett. 50 (2009) 5589–5595.
[46] C.M. Nunes, A.L. Monteiro, J. Braz. Chem. Soc. 18 (2007) 1443–1447.
[47] W. Zawartka, A. Gniewek, A.M. Trzeciak, J.J. Ziolkowski, J. Pernak, J. Mol. Catal. A: Chem. 304 (2009) 8–15.
[48] J. Lindh, P.J.R. Sjöberg, M. Larhed, Angew. Chem., Int. Ed. 49 (2010) 7733–7737.
[49] M. Tromp, J.R.A. Sietsma, S.A. van Bokhoven, G.P.F. van Strijdonck, R.J. van Haaren, A.M.J. van der Eerden, P.W.N.M. van Leewen, D.C. Koningsberger, Chem. Commun. (Cambridge) (2003) 128–129.
[50] D. Harakat, J. Muzart, J. Le Bras, RSC Adv. 2 (2012) 3094–3099.
[51] R.S. Paton, J.M. Brown, Angew. Chem., Int. Ed. 51 (2012) 10448–10450.
[52] W. Zhu, H. Wang, H. Peng, G. Liu, Y. Guo, Chin. J. Chem. 31 (2013) 371–376.
[53] M. Parera, A. Dachs, M. Solà, A. Pla-Quintana, A. Roglans, Chem. Eur. J. 18 (2012) 13097–13107.
[54] S.-W. Cheng, M.-C. Tseng, K.-H. Lii, C.-R. Lee, S.-G. Shyu, Chem. Commun. (Cambridge) 47 (2011) 5599–5601.
[55] W. Henderson, C. Evans, Inorg. Chim. Acta 294 (1999) 183–192.
[56] J.M. Brown, K.K. Hii, Angew. Chem., Int. Ed. Engl. 35 (1996) 657–659.
[57] L. Ripa, A. Hallberg, J. Org. Chem. 61 (1996) 7147–7155.
[58] M.A. Aramendia, F. Lafont, M. Moreno-Manas, R. Pleixats, A. Roglans, J. Org. Chem. 64 (1999) 3592–3594.
[59] A. Pla-Quintana, A. Roglans, Arkivoc 2005 (2005) 51–62.
[60] T.d.A. Fernandes, V.B. Gontijo, M.N. Eberlin, A.J.M. da Silva, P.R.R. Costa, J. Org. Chem. 75 (2010) 7085–7091.
[61] C.D. Buarque, V.D. Pinho, B.G. Vaz, M.N. Eberlin, A.J.M. da Silva, P.R.R. Costa, J. Organomet. Chem. 695 (2010) 2062–2067.
[62] D. Agrawal, D. Schröder, C.M. Frech, Organometallics 30 (2011) 3579–3587.
[63] L.S. Santos, G.B. Rosso, R.A. Pilli, M.N. Eberlin, J. Org. Chem. 72 (2007) 5809–5812.
[64] J. Zhou, W. Tang, Y. Guo, Y. Ding, Chin. J. Chem. 27 (2009) 1733–1740.
[65] E. Thiery, C. Chevrin, J. Le Bras, D. Harakat, J. Muzart, J. Org. Chem. 72 (2007) 1859–1862.
[66] H. Guo, R. Qian, Y. Liao, S. Ma, Y. Guo, J. Am. Chem. Soc. 127 (2005) 13060–13064.
[67] J.A. Kenny, M. Wills, K. Versluis, A.J.R. Heck, T. Walsgrove, Chem. Commun. (Cambridge) (2000) 99–100.
[68] R. Noyori, S. Hashiguchi, Acc. Chem. Res. 30 (1997) 97–102.
[69] C. Adlhart, P. Chen, Helv. Chim. Acta 83 (2000) 2192–2196.
[70] H.-Y. Wang, W.-L. Yim, T. Klüner, J.O. Metzger, Chem. Eur. J. 15 (2009) 10948–10959.
[71] H. Wang, J.O. Metzger, Organometallics 27 (2008) 2761–2766.
[72] H.-Y. Wang, W.-L. Yim, Y.-L. Guo, J.O. Metzger, Organometallics 31 (2012) 1627–1634.
[73] S. Kurzhals, C. Enders, W.H. Binder, Macromolecules 46 (2013) 597–607.
[74] A.O. Aliprantis, J.W. Canary, J. Am. Chem. Soc. 116 (1994) 6985–6986.
[75] R. Colton, J.C. Traeger, Inorg. Chim. Acta 201 (1992) 153–155.
[76] I. Ahmed, A.M. Bond, R. Colton, M. Jurcevic, J.C. Traeger, J.N. Walter, J. Organomet. Chem. 447 (1993) 59–65.
[77] D.J.F. Bryce, P.J. Dyson, B.K. Nicholson, D.G. Parker, Polyhedron 17 (1998) 2899–2905.
[78] C. Decker, W. Henderson, B.K. Nicholson, J. Chem. Soc., Dalton Trans. (1999) 3507–3513.
[79] C. Hinderling, C. Adlhart, P. Chen, Angew. Chem., Int. Ed. 37 (1998) 2685–2689.
[80] C. Adlhart, C. Hinderling, H. Baumann, P. Chen, J. Am. Chem. Soc. 122 (2000) 8204–8214.
[81] P. Chen, Angew. Chem., Int. Ed. 42 (2003) 2832–2847.
[82] T.A. Kirkland, D.M. Lynn, R.H. Grubbs, J. Org. Chem. 63 (1998) 9904–9909.
[83] B. Mohr, D.M. Lynn, R.H. Grubbs, Organometallics 15 (1996) 4317–4325.
[84] C.H. Beierlein, B. Breit, S.R.A. Paz, D.A. Plattner, Organometallics 29 (2010) 2521–2532.
[85] F.F.D. Oliveira, M.R. dos Santos, P.M. Lalli, E.M. Schmidt, P. Bakuzis, A.A.M. Lapis, A.L. Monteiro, M.N. Eberlin, B.A.D. Neto, J. Org. Chem. 76 (2011) 10140–10147.
[86] M.A. Schade, J.E. Fleckenstein, P. Knochel, K. Koszinowski, J. Org. Chem. 75 (2010) 6848–6857.
[87] N.J. Farrer, R. McDonald, J.S. McIndoe, Dalton Trans. (2006) 4570–4579.
[88] D.M. Chisholm, A.G. Oliver, J.S. McIndoe, Dalton Trans. 39 (2010) 364–373.
[89] S.M. Jackson, D.M. Chisholm, J.S. McIndoe, L. Rosenberg, Eur. J. Inorg. Chem. 2011 (2011) 327–330.
[90] E. Crawford, T. Lohr, E.M. Leitao, S. Kwok, J.S. McIndoe, Dalton Trans. 2009 (2009) 9110–9112.
[91] H. Takahashi, T. Hayakawa, M. Ueda, Chem. Lett. 29 (2000) 684–685.
[92] K.L. Vikse, S. Kwok, R. McDonald, A.G. Oliver, J.S. McIndoe, J. Organomet. Chem. 716 (2012) 252–257.
[93] N.J. Farrer, K.L. Vikse, R. McDonald, J.S. McIndoe, Eur. J. Inorg. Chem. 2012 (2012) 733–740.
[94] L.S. Santos, Eur. J. Org. Chem. 2008 (2008) 235–253.
[95] L.S. Santos, in: L.S. Santos (Ed.), Reactive Intermediates: MS Investigations in Solution, Wiley-VCH Verlag GmbH & Co. KGaA, Weinheim, 2010, pp. 133–198.
[96] J. Hyvl, D. Agrawal, R. Pohl, M. Suri, F. Glorius, D. Schröder, Organometallics 32 (2013) 807–816.
[97] E.F. Wilson, H.N. Miras, M.H. Rosnes, L. Cronin, Angew. Chem., Int. Ed. 50 (2011) 3720–3724.
[98] K.L. Vikse, M.P. Woods, J.S. McIndoe, Organometallics 29 (2010) 6615–6618.
[99] J. Luo, A.G. Oliver, J.S. McIndoe, Dalton Trans. 42 (2013) 11312–11318.
[100] K.L. Vikse, Z. Ahmadi, C.C. Manning, D.A. Harrington, J.S. McIndoe, Angew. Chem., Int. Ed. 50 (2011) 8304–8306.
[101] Z. Ahmadi, J.S. McIndoe, Chem. Commun. (Cambridge) 49 (2013) 11488–11490.
[102] M.A. Henderson, J. Luo, A. Oliver, J.S. McIndoe, Organometallics 30 (2011) 5471–5479.
[103] Z. Ahmadi, A.G. Oliver, J.S. McIndoe, ChemPlusChem 78 (2013) 632–635.